

1-1-2017

The Effect Of Acetylation Of Cytochrome C On Its Functions In Prostate Cancer

Viktoriia Bazylanska
Wayne State University,

Follow this and additional works at: https://digitalcommons.wayne.edu/oa_theses

 Part of the [Biochemistry Commons](#), [Genetics Commons](#), and the [Molecular Biology Commons](#)

Recommended Citation

Bazylanska, Viktoriia, "The Effect Of Acetylation Of Cytochrome C On Its Functions In Prostate Cancer" (2017). *Wayne State University Theses*. 550.
https://digitalcommons.wayne.edu/oa_theses/550

This Open Access Thesis is brought to you for free and open access by DigitalCommons@WayneState. It has been accepted for inclusion in Wayne State University Theses by an authorized administrator of DigitalCommons@WayneState.

**THE EFFECT OF ACETYLATION OF CYTOCHROME C ON ITS FUNCTIONS IN
PROSTATE CANCER**

by

VIKTORIA ROSTYSLAVIVNA BAZYLIANSKA

THESIS

Submitted to the Graduate School of

Wayne State University,

Detroit, Michigan

In partial fulfilment of the requirements

For the degree of

MASTER OF SCIENCE

2017

MAJOR: BIOCHEMISTRY AND

MOLECULAR BIOLOGY

Approved by:

Advisor

Date

©COPYRIGHT BY
VIKTORIA ROSTYSLAVIVNA BAZYLIANSKA
2017
All Rights Reserved

DEDICATION

Every achievement requires hard work, self-motivation, dedication, and the loving support of beloved people. I dedicate my work and efforts to all who believed in me through my whole educational path.

I dedicate my master's thesis and give special thanks to my dear mother, whose love, affection, and encouragement I felt from afar. Her daily prayers give me strength, patience, the desire to persevere my life goals. Thank you for never losing trust and faith in me.

I dedicate this work to my loving and esteemed grandparents, whose wisdom inspires and guides me to great achievements. They inspire me to be the very best I can be, and teach me to never give up. I am infinitely grateful for all lessons, efforts, and patience they have done to make me who I am.

I dedicate this work to my dear brother and all my cherished friends who have always been with me through my ups and downs, cheering me up and giving the energy to keep going.

There are not enough words and explanations to express my gratefulness, my love, and how glad I am to have you as my family. Thank you for everything.

ACKNOWLEDGEMENTS

The Master's Program in Biochemistry and Molecular Biology at Wayne State University, School of Medicine gave me an essential opportunity not only to gain relevant theoretical knowledge, to receive hands-on practical experience, and to master advanced methods, but also to enhance my career skills. I would like to take this opportunity to express my sincere gratitude to all the people and educational programs for making my graduate school possible.

I would like to express my special thanks of gratitude to my academic advisor, Dr. Maik Hüttemann, who shared his vast research experience, taught me how to think scientifically, and helped me design experiments. He taught me how to become an independent researcher, a better writer, and an excellent presenter. Dr. Hüttemann has always been very friendly, tactful, and understanding with me. I am very happy for being able to be a part of his lab.

I am very grateful to the Fulbright Graduate Student Program for the unique opportunity to study in one of the best medical schools in the US, and to work in innovative scientific centers which conduct the most advanced research. International experience and cross cultural integration not only provided the opportunity to strengthen my leadership and organizational skills, to interact and collaborate with people who have a different mentality, but also helped me to develop the skills necessary to live, study, and work efficiently in cultures other than my own.

I would also like to express my deep gratitude to my committee, Dr. Brian Edwards, and Dr. Ladislau Kovari for their invaluable project guidance. They have been truly understanding, flexible and supportive, providing the right balance of encouragement and constructive criticism. I am also very thankful to Dr. Brian Edwards for his help with protein crystallization. I would like to extend my gratitude to Dr. Siddhesh Aras who has been of great assistance, sharing his

knowledge and experience, teaching innovative techniques, and offering invaluable research and project advice.

Many thanks to the best lab team ever, my dear friends, Ms. Jenney Liu, Dr. Alemu Fite, Dr. Mallika Somayajulu, Dr. Maurice Recanati, Ph.D. students Hasini Kalpage, Stephanie Gladysck, and Neeraja Purandare for their support and for a great time spent in the lab. I sincerely thank Ms. Asmita Vaishnav for helping me operate the French Cell Press and bacterial protein purification. I hope that we all will remain in contact for many years.

I wish to express my deepest sense of gratitude to all my friends here and abroad, and last but not least to my beloved family especially my mother who has always supported me. My family has always believed in me and supported all my plans, my beginnings and achievements. My dear heart mother always encouraged me in my endeavors and rejoiced in my achievements. She told me that my choice, to follow a scientific path, will help many people to live better, and for such a noble goal, it is worth to live and work hard.

TABLE OF CONTENTS

Dedication.....	iii
Acknowledgements.....	iv
Lists of Figures.....	x
List of Tables.....	xii
CHAPTER 1: INTRODUCTION.....	1
1.1 Mitochondria: It is All About Energy and Free Radicals.....	1
1.2 Mitochondrial Protein Cytochrome <i>c</i> Plays an Essential Role in Mitochondrial Function.....	3
1.3 The Origin of Cytochrome <i>c</i>	4
1.4 The Structure of Cytochrome <i>c</i>	5
1.5 The Functions of Cytochrome <i>c</i>	7
1.5.1 The Role of Cytochrome <i>c</i> in Respiration and Energy Production.....	7
1.5.2 The Role of Cytochrome <i>c</i> in the Programmed Cell death.....	8
1.5.3 Cytochrome <i>c</i> as a Radical Scavenger and Producer.....	10
1.5.4 Cytochrome <i>c</i> Catalyzes Cardiolipin Oxidation.....	12
1.5.5 Cytochrome <i>c</i> Plays Role in Redox-Coupled Protein Import via Erv1- Mia40.....	13
1.6 Regulation of Cytochrome <i>c</i> and Other Mitochondrial Proteins by Post-Translational Modifications.....	14
1.6.1 Phosphorylation of Cytochrome <i>c</i> Regulates Respiration and Apoptosis...	14
1.6.2 Methylation of Lysine Residues of Cytochrome <i>c</i>	17

1.6.3 Mitochondrial Lysine Acetylation.....	18
1.7 Mitochondrial Acetylation in Human Diseases.....	19
1.7.1 Mitochondrial Protein Hyperacetylation in the Failing Heart.....	20
1.7.2 Impact of Acetylation on the Neurodegenerative Diseases.....	21
1.7.3 Acetylation of Lysine Residues in Cancer Metabolism.....	22
1.8 Prostate Cancer.....	23
1.9 Metabolic Shift in Cancer: the Warburg Effect.....	25
 CHAPTER 2: THE EFFECT OF ACETYLATION OF CYTOCHROME <i>c</i> ON ITS FUNCTIONS IN CANCER.....	 28
2.1 Background and Purpose of Study.....	28
2.2 Materials and Methods.....	30
2.2.1 Generation of Cytochrome <i>c</i> Variants.....	30
2.2.2 Bacterial Overexpression of Cytochrome <i>c</i> Variants.....	34
2.2.3 Western Blotting Analyses of the Overexpressed Cytochrome <i>c</i>	35
2.2.4 Purification of Cytochrome <i>c</i> Variants.....	36
2.2.5 Analysis of Cytochrome <i>c</i> Absorption Spectra.....	37
2.2.6 Determination of the Concentration of Cytochrome <i>c</i> Variants.....	37
2.2.7 Mass Spectrometry of Castrate-Resistant and Castrate-Sensitive Prostate Tumor Xenografts to Detect Site-Specific Acetylation.....	38
2.2.8 Caspase- 3 Activity Induction by Cytochrome <i>c</i> Variants.....	38
2.2.9 Cytochrome <i>c</i> Oxidase Activity Measurements.....	39
2.2.10 Measurement of Cytochrome <i>c</i> Redox Potential.....	40
2.2.11 Measurement of Rates of Oxidation and Reduction.....	41

2.2.12. Measurement of Peroxidase Activity of Cytochrome <i>c</i> Mutants.....	42
2.2.13 Crystallization of Cytochrome <i>c</i> Variants.....	42
2.2.14 Cell Culture.....	43
2.2.15 Transient Transfection and Selection of Double Knockout Mouse Lung Fibroblasts.....	43
CHAPTER 3: RESULTS.....	45
3.1 Cytochrome <i>c</i> is Acetylated on Lys53 in Prostate Cancer Xenografts.....	45
3.2 Sequence Confirmation of Cytochrome <i>c</i> mutants.....	47
3.3 Transient Transfection of Double Knockout Mouse Lung Fibroblasts.....	49
3.4 Cytochrome <i>c</i> Variants were Overexpressed in <i>E. coli</i>	49
3.5 Concentration Determination and Purification of Functional and Correctly Folded Cytochrome <i>c</i> Variants from <i>Escherichia coli</i>	51
3.6 Acetylmimetic Lys53Gln Cytochrome <i>c</i> Mutant Exhibits a Decrease in Respiration Rate with Isolated Cytochrome <i>c</i> Oxidase.....	52
3.7 Acetylmimetic Lys53Gln Cytochrome <i>c</i> is Incapable to Activate Caspase-3, and Turns off Apoptosis.....	54
3.8 Assessments of Peroxidase Activity of Cytochrome <i>c</i> Mutants.....	55
3.9 Measurement of Redox Potential of Cytochrome <i>c</i> Mutants	57
3.10 Measurement of Rates of Oxidation and Reduction of Cytochrome <i>c</i> Mutants...58	
3.11 Crystallization of Cytochrome <i>c</i> Variants.....	59
CHAPTER 4: SUMMARY.....	65
4.1 Discussion and Conclusion.....	65
4.2 Future Directions.....	68

REFERENCES.....70
ABSTRACT77
AUTOBIOGRAPHICAL STATEMENT.....79

LIST OF FIGURES

Figure 1. Ribbon model of horse cytochrome <i>c</i>	6
Figure 2. Absorption and CD spectra of cytochrome <i>c</i> -554 from <i>Methylosinus trichosporium</i> OB3b.....	6
Figure 3. The intrinsic, or mitochondrial type II apoptosis.....	10
Figure 4. The importance and the diversity of PTMs of lysine residue among mitochondrial proteins.....	19
Figure 5. Healthy prostate and prostate cancer.....	25
Figure 6. Metabolic shift in cancer cells - the Warburg effect.....	26
Figure 7. Model of cytochrome <i>c</i> regulation.....	29
Figure 8. pLWO1 expression vector.....	31
Figure 9. pBABE-puro expression vector.....	31
Figure 10. Overview of the QuickChange II site-directed mutagenesis method.....	32
Figure 11. Expression and purification of cytochrome <i>c</i> variants.....	37
Figure 12. Hansatech Oxygraph Plus System connected to a water bath.....	40
Figure 13. Nano-LC/ESI/MS/MS spectrum of TGQAPGYSYTAANK <u>N</u> KNK.....	45
Figure 14. Cytochrome <i>c</i> sequence alignment reveals that Lys-53 is conserved in mammals...	46
Figure 15. Ribbon model of cytochrome <i>c</i>	46
Figure 16. Sequence confirmation of pLWO1 cytochrome <i>c</i> constructs.....	48
Figure 17. Sequence confirmation of pBABE cytochrome <i>c</i> constructs.....	48
Figure 18. Western blot analysis of the double knockout mouse lung fibroblasts.....	49

Figure 19. Overexpression of Lys53Gln cytochrome <i>c</i> after 0, 2, 4, and 6 hours IPTG induction.....	50
Figure 20. Western blot analysis of the overexpressed Lys53Gln cytochrome <i>c</i> after 2, 4, and 6 hours of IPTG induction.....	50
Figure 21. Bacterial pellets of the overexpressed Lys53Gln cytochrome <i>c</i>	51
Figure 22. Purified cytochrome <i>c</i> mutant’s absorption spectra.....	52
Figure 23. Measurements of Cytochrome <i>c</i> oxidase activity with purified cytochrome <i>c</i> mutants.....	53
Figure 24. The ability to trigger downstream caspase-3 activation is strongly inhibited in the cytochrome <i>c</i> acetylmimetic Lys53Gln and nonpolar control Lys53Ile mutants <i>in vitro</i>	55
Figure 25. Peroxidase activity of the cytochrome <i>c</i> variants.....	56
Figure 26. Measurement of cytochrome <i>c</i> mutant’s redox potential.....	57
Figure 27. Cytochrome <i>c</i> variants’ oxidation rate.....	58
Figure 28. Cytochrome <i>c</i> variants’ reduction rate.....	59
Figure 29. Crystal of the Lys53Gln cytochrome <i>c</i> mutant.....	60
Figure 30. The comparison of the “omit” density for the Lys53Gln in the two cytochrome <i>c</i> molecules in the asymmetric unit of the crystal structure.....	60
Figure 31. The structure of Lys53Gln cytochrome <i>c</i> is superposed onto the native mouse/rat cytochrome <i>c</i> (5C0Z.pdb) using chain-A in both structures.....	61

LIST OF TABLES

Table 1. Classification and characteristics of cytochrome <i>c</i>	5
Table 2. Designed primers for the QuickChange II site-directed mutagenesis protocol.....	33
Table 3. Crystallographic data summarizing and comparing three structures of mouse / rat cytochrome <i>c</i> : Native, K53Q, and human Y46F.....	62

CHAPTER 1

INTRODUCTION

1.1 Mitochondria: It is All About Energy and Free Radicals

The mitochondrion is a cellular power generator that supplies metabolism with different molecular building blocks and energy in a form of adenosine triphosphate (ATP) for movement and growth. It is a double membrane organelle found in the cytoplasm of all eukaryotic organisms. The outer mitochondrial membrane covers the organelle and is 60 to 75 Angstroms (\AA) thick. The membrane is freely permeable to small molecules and contains many special channels, formed by the integral protein porin, for the transport of large molecules. The inner membrane forms numerous folds and creates layered structures, called cristae. Compared to the outer membrane, the inner membrane is much less permeable and more selective. The inner membrane is rich in a mitochondria-specific phospholipid, cardiolipin, that contains four fatty acid chains and plays a role in membrane impermeability. The space between the outer membrane and the inner membrane is called the intermembrane space. One protein that is localized in the intermembrane space is Cytochrome *c* (*Cytc*), an electron carrier that plays an essential role in the electron transport chain (ETC). The compartment enclosed by the inner membrane, called the matrix, contains a large number of mitochondrial proteins and enzymes. Mitochondria are unique organelles; they have their own DNA and their own ribosomes, which can be found in the matrix. Human circular mtDNA contains 16,569 bp and encodes 2 rRNAs, 22 tRNAs, and 13 proteins. In humans, mitochondria are inherited maternally.

The primary function of mitochondria is to generate ATP through respiration, and to regulate cellular metabolism. Most of the energy released from the breakdown of carbohydrates or

lipids is derived by oxidative phosphorylation (OXPHOS), a process of ATP formation by a series of electron carriers that takes place inside mitochondria. In the inner mitochondrial membrane, these carriers constitute the ETC and comprise four membrane-bound complexes: NADH dehydrogenase (complex I), succinate dehydrogenase (complex II), the non-protein electron carrier ubiquinone, *bc*₁-complex (complex III), Cyt_c, cytochrome *c* oxidase (COX; complex IV), and ATP synthase that generates ATP. During oxidative phosphorylation, electrons are transferred from electron donors (NADH and FADH₂) to a terminal electron acceptor (O₂) via a series of oxidation-reduction reactions. In the ETC, two electrons from oxidized NADH, a product of the Krebs cycle, enter the ETC at complex I. These electrons are transferred from NADH to flavin mononucleotide followed by transfer through Fe-S clusters to coenzyme Q (ubiquinone). Ubiquinone, a small lipid-soluble molecule, in turn, passes electrons from complex I to complex III. Electrons are transferred from cytochrome *c*₁ to Cyt_c, a small globular heme protein that carries a single electron from complex III to complex IV. At the end of the chain, COX passes electrons to the final electron acceptor, a molecule of oxygen, which is reduced to water. In parallel to complex I, complex II accepts electrons from succinate, a citric acid cycle intermediate. Electrons are transferred to coenzyme Q through the electron donor FADH₂, and then to complex III and IV as described above. Passage of electrons through the ETC releases energy which creates a proton gradient. This gradient creates a mitochondrial membrane potential ($\Delta\Psi_m$) across the inner mitochondrial membrane by actively "pumping" protons into the intermembrane space via complexes I, III, and IV. The generated transmembrane proton gradient is used to produce free energy and drives the phosphorylation of ADP (adenosine diphosphate) to ATP. It has long been known that $\Delta\Psi_m$ is also directly linked to free radical production. Under healthy conditions, $\Delta\Psi_m$ is maintained around 120 mV which is sufficient for efficient generation of ATP (Kaim and

Dimroth, 1999). The production of reactive oxygen species (ROS) increases exponentially when the level of $\Delta\Psi_m$ exceeds reach 140 mV (Liu, 1999).

There is a small percentage of electrons (0.1–2%) that do not complete their pathway in the ETC and directly leak to oxygen, partially reducing oxygen to the superoxide anion ($O_2^{\bullet-}$). Electron leakage takes place when electrons passing through the ETC exit prior to the reduction of oxygen to water at COX. Complexes I, III, and ubiqui-semiquinol are the main mitochondrial radical sources. Complex I is a major site of the production of mitochondrial ROS *in vivo*, and complex III is considered a minor source of superoxide (Jastroch et al., 2010).

Electrons reacting with oxygen cause the production of free-radical superoxide, a highly reactive molecule. Although superoxide is a weak oxidant, it is a precursor for other ROS. Superoxide can be dismutated to hydrogen peroxide, which in turn may be fully reduced to H_2O or partially reduced to hydroxyl radical (OH^{\bullet}), a powerful oxidant. Superoxide can also react with nitric oxide (NO^{\bullet}) to produce peroxynitrite which is one of the strongest oxidants (Beckman and Koppenol, 1996). Superoxide plays an essential role in oxidative stress. A high concentration of superoxide causes oxidative damage to proteins, lipids, and DNA due to their high reactivity towards such cellular compounds. The accumulation of damage can lead to mitochondrial dysfunction that has been implicated in many diseases such as cancer, neurodegenerative disease, heart failure, and aging.

1.2 Mitochondrial Protein Cytochrome *c* Plays an Essential Role in Mitochondrial Function

Cytochrome *c* (Cyt c) is a small, 12.4 kDa globular multifunctional heme protein which is involved in cell life and death decision making processes. In humans and other mammalian species the mature Cyt c contains 104 amino acids. Compared to other cytochrome proteins, Cyt c is highly

water-soluble and positively charged ($pI = 9.6$). *Cytc* is conserved in many species, including plants, animals, and unicellular organisms. The sequences of human and chimpanzee *Cytc* are identical and differ from those of other mammals by only several amino acids (Hüttemann et al., 2003).

Cytc is located in the mitochondrial intermembrane space under normal conditions, and is encoded by the nuclear gene *CYCS* in human (Lee et al., 2006). The protein is synthesized as an inactive precursor, called apocytochrome *c*, and translated in the cytoplasm. During the translocation to the mitochondria, the heme group is covalently attached to cysteines 14 and 17 of side chains of the protein via thioether bonds. The heme iron exists in a hexacoordinate configuration comprising four nitrogen atoms in the heme and the His 18 and Met-80 residues.

1.3 The Origin of Cytochrome *c*

Cytc was first discovered in 1884 by MacMunn. His microspectroscopic studies on tissue samples from different organisms suggested that heme proteins play a crucial role in cellular respiration. McMunn named the pigment from muscles myothaematin and histohaematin from other tissues. His discovery demonstrates that the mechanism of energy production takes place in tissue and cells. Later, respiratory pigments were rediscovered in 1925 by David Keilin, who renamed them as cytochromes, or “cellular pigments”. He discovered that heme proteins were present not only in plants and animals, but also in yeast and bacteria. David Keilin believed that *Cytc* could function as an electron carrier by undergoing oxidation-reduction reactions as it contains a Fe atom. Thereby, he proposed a model for the basics of the respiratory chain, or ETC. Based on their lowest energy absorption band position in the reduced state, he classified these

proteins as cytochromes *a* (605 nm), *b* (~565 nm), and *c* (550 nm). The further classification of Cyt*c* was done later, in 1991 by R. P. Ambler (Table 1).

Table 1. Classification and characteristics of Cytochrome *c*

Class	Characteristics
I	Mitochondrial and bacterial lowspin soluble Cyt <i>c</i> . The heme-attachment site is towards the N-terminus of the His residue, and the sixth ligand provided by a Met is towards the C-terminus.
II	Compared to the class I, it is a high spin Cyt <i>c</i> , which has the heme-attachment site close to the N-terminus of His residue.
III	The class includes the low redox potential multiple-heme cytochromes. The heme <i>c</i> groups are structurally and functionally nonequivalent. The group presents a vast range of redox potentials from 0 to -400 mV.
IV	This group includes the protein complexes which have other prosthetic groups in addition to heme <i>c</i> .

1.4 The Structure of Cytochrome *c*

One of the first crystalized proteins was Cyt*c* from horse heart. The Cyt*c* heme prosthetic group is covalently attached to the protein via two thioether bonds to cysteine residues. The conjugated ring system (Figure 1) of the heme group that surrounds a Fe ion allows the electrons to be very mobile. The iron ion interconverts between Fe²⁺ (reduced) and Fe³⁺ (oxidized) states, therefore, Cyt*c* is able to perform oxidation and reduction reactions.

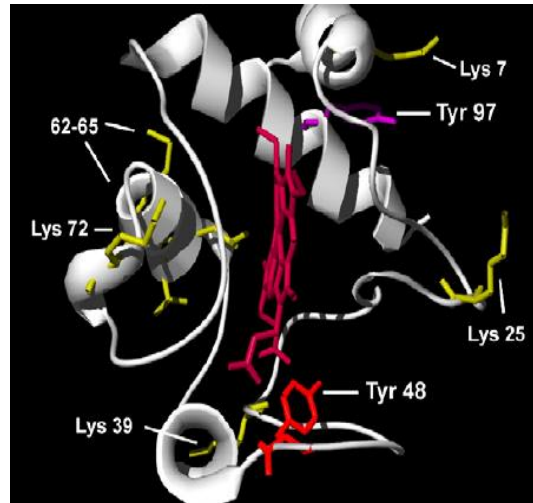


Figure 1. Ribbon model of horse cytochrome *c*. The heme group is shown in dark red. Essential amino acids for Apaf-1 binding and activation of caspase are shown in yellow. The picture is taken from (Yu et al., 2008).

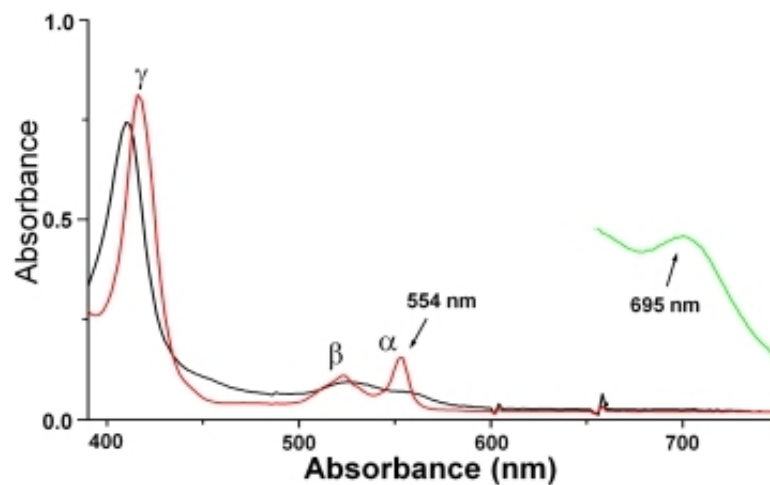


Figure 2. Absorption and CD spectra of cytochrome *c*-554 from *Methylosinus trichosporium* OB3b. In the reduced spectrum, the α -band has a maximum absorbance at 554 nm. In the oxidized spectrum, a characteristic 695 nm absorption band indicates the ligation of Met-80 to the heme group. This band is called a “marker of Cyt*c* integrity”. The picture is taken from (Harbitz and Andersson, 2011).

Methionine 80 and Histidine 18 coordinate the iron of the heme group. The bond between the iron of the heme group and Met-80 residue results in a weak 695 nm absorption band in the oxidized Cyt c spectrum (Figure 2). This peak called as an “indicator of trouble” (Dickerson and Timkovich, 1975) since it is usually lost at any harmful treatment, and the lack of which suggests that the protein folded incorrectly.

1.5 The Functions of Cytochrome c

The functional importance of Cyt c has long been recognized and it has been widely investigated in more than 20,000 studies. Cyt c is an essential protein as it is involved in cellular life and death decisions. As part of the mitochondrial ETC Cyt c is essential for electron transfer and the energy production process. It plays a crucial role in apoptosome formation and the progression of programmed cell death. Cyt c also participates in cardiolipin peroxidation, ROS scavenging and formation, regulation of cell signaling pathways, and redox coupled protein import (Hüttemann et al., 2011; Kagan et al., 2005; Li et al., 2000a; Pecina et al., 2010).

1.5.1 The Role of Cytochrome c in Respiration and Energy Production

Energy is essential to life and all living organisms. ATP is a high-energy molecule and considered as the energy currency of life. ATP contains adenosine and three phosphates with high-energy bonds, the breakdown of which liberates energy for all biological processes. On average, a 70-kg person makes about 40 kg of ATP per day. About 90% of cellular ATP is generated by the OXPHOS machinery, which is located in the inner mitochondrial membrane and consists of the ETC and ATP synthase. During electron transfer in the ETC, complexes I (NADH dehydrogenase), III (bc_1 complex), and IV (cytochrome c oxidase, COX) pump protons from the

matrix into the intermembrane space, generating the mitochondrial membrane potential ($\Delta\Psi_m$). ATP synthase (complex V) uses the membrane potential to drive the phosphorylation of ADP to ATP (Stock et al., 1999).

In the final step of ETC, Cyt c functions as a single electron carrier between complex III and IV. Four electrons are required to reduce a molecule of oxygen to water which is accompanied by a free energy change of $\Delta G_o' = -100$ kJ/mol (Hinkle et al., 1991). Under physiological conditions, this reaction is the rate-limited step of the ETC (Acin-Perez et al., 2003; Dalmonte et al., 2009; Villani and Attardi, 1997; Villani et al., 1998) and fundamental for the generation cellular energy in the form of ATP. Consequently, Cyt c is essential for aerobic energy production and Cyt c knockout mice die around midgestation, when a switch from glycolysis to respiration occurs (Li et al., 2000b).

1.5.2 The Role of Cytochrome *c* in the Programmed Cell death

Cyt c plays a second role in type II (intrinsic) apoptosis. For the first time, the importance of Cyt c in the apoptotic pathway was demonstrated in a cell-free apoptotic system in 1996 by Liu et al. (Liu et al., 1996). Another study suggested that Cyt c undergoes molecular changes during programmed cell death (Krippner et al., 1996).

Apoptosis, or programmed cell death, is an essential physiological mechanism that plays a crucial role in developing and maintaining the health of an organism, eliminating old and unhealthy cells. There are two main apoptotic pathways: type I - the extrinsic or death receptor pathway, and type II - the intrinsic or mitochondrial pathway. In the intrinsic apoptotic pathway, intracellular stress transduces signals to the mitochondria to release apoptogenic factors into the cytosol and initiate programmed cell death (Figure 3). The BCL-2 family protein is involved in the regulation

of apoptosis, pro-and anti-apoptotic proteins activate and inhibit apoptosis, respectively. Pro-apoptotic members of Bcl-2 family proteins, such as Bax and Bak, acting on the mitochondrial permeability transition pore (mPTP), trigger the release of mitochondrial apoptogenic factor *Cytc* into the cytosol, leading to caspase activation. After entering the cytoplasm, *Cytc* binds to apoptotic protease-activating factor 1 (Apaf-1), which results in an increased affinity of the complex for dATP. This binding is crucial for the formation of the apoptosome (Wang, 2001). The apoptosome in turn recruits procaspase-9, initiating its cleavage to an active form. Activated caspase-9 then acts as the cleavage factor of caspase-3 (Green, 2000).

Hundreds of studies have demonstrated the essential role of *Cytc* in apoptosis. In 2000, Li et al. confirmed that *Cytc* is crucial for caspase activation. Using cell lines null for *Cytc*, it was shown that caspase-3 activity was reduced when stimulated with apoptosis-inducing agents (Li et al., 2000a). A recent study has reported that *Cytc* Lys72 is critical for apoptosis (Hao et al., 2005). A mouse model with a Lys72Ala mutation had healthy respiration but was unable to initiate oligomerization of Apaf-1, and thus, was deficient in healthy apoptotic function. The Lys72Ala mutant mice were embryonic lethal (Hao et al., 2005). In 2000, Kluck et al. confirmed that in cell-free systems, trimethylation of *Cytc* Lys72 inhibits the ability of the protein to activate caspases while maintaining normal oxidative phosphorylation level (Kluck et al., 2000).

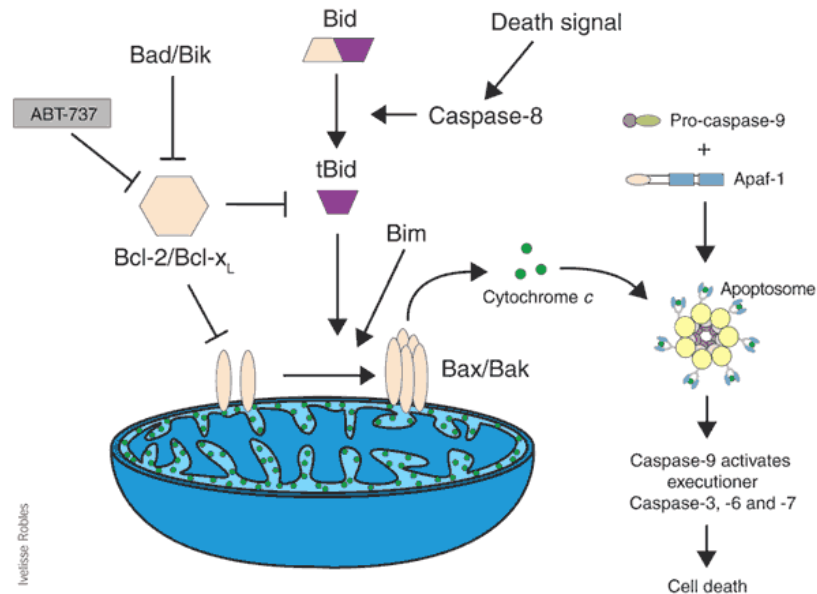


Figure 3. The intrinsic, or mitochondrial type II apoptosis. The intrinsic apoptotic pathway involves the release of the apoptosis-triggering *Cytc* into the cytosol, binding to Apaf-1, and activation of caspase cascade. The picture is taken from (Wagner, 2005).

1.5.3 Cytochrome *c* as a Radical Scavenger and Producer

Oxygen is essential to humans and all other obligate aerobic organisms. Oxygen is required for the breakdown of complex food molecules into simpler substances and for the conversion of their stored energy into ATP. During normal mitochondrial oxidative metabolism, electron transfer reactions with oxygen that occur at the ETC complexes generate toxic byproducts - ROS, including superoxide ($O_2^{\bullet-}$), hydrogen peroxide (H_2O_2), and hydroxyl radicals ($\bullet OH$) (Cadenas and Davies, 2000; Kadenbach et al., 2004). ROS is generated mostly by complex I which releases them into the matrix, complex III that primarily releases ROS into the intermembrane space, and by the reduced ubiquinol pool (Han et al., 2003; Han et al., 2001; Turrens et al., 1985). ROS are highly reactive and can damage DNA or RNA, oxidize polyunsaturated fatty acids in lipids and amino

acids in proteins. Thus, ROS play an important role in pathogenesis of different diseases, such as neurodegenerative and cardiovascular diseases, ischemia reperfusion injury, and aging.

Aerobic organisms have integrated antioxidant systems that can neutralize the toxic effects of ROS and protect an organism. The main enzymatic antioxidants are superoxide dismutase (SOD), catalase, and glutathione peroxidase (GSH-Px). There are three forms of SOD, CuZn-SOD, EC-SOD, and mitochondrial Mn-SOD. The superoxide molecules are reduced to hydrogen peroxide by SOD. H_2O_2 produced by the action of SOD is further reduced to a molecule of water by catalase and the GSH-Px.

Free Cyt c is capable of functioning as a radical scavenger within the inner-membrane space (Korshunov et al., 1999). The enzyme can regenerate O_2 by removing the unpaired electron (Pereverzev et al., 2003). These electrons can be transported to COX for ATP production and regenerate the oxidized form of Cyt c . Both the reduced and oxidized form of Cyt c can function as a hydrogen peroxide scavenger (Wang et al., 2003).

Furthermore, Cyt c can produce ROS. p66^{Shc} is one of three isoforms of ShcA (Src homologous- collagen homologue) adaptor protein family together with p46^{Shc} and p52^{Shc}. p66^{Shc} is a small protein (66 kDa) that mostly localized in mitochondria where it alters mitochondrial function (Nemoto et al., 2006). p66^{Shc} regulates the generation of ROS, induction of apoptosis, and lifespan in mammals. The protein's functions are regulated via reversible phosphorylation (Pinton et al., 2007). During cellular stress, receiving an electron from Cyt c , p66 is reduced and generates hydrogen peroxide (Giorgio et al., 2005). The production of ROS via the p66^{Shc} apoptotic pathway contributes to the increased levels of peroxide that is essential for cardiolipin peroxidation by Cyt c . Cardiolipin peroxidation is critical for the release of Cyt c into the cytosol during the apoptosis. The release of Cyt c from the mitochondria correlates with the production of H_2O_2 by p66^{Shc} (Sun

et al., 2010), and could be an important switch utilized by a cell as an initiating event of apoptosis (Liu, 1999).

1.5.4 Cytochrome *c* Catalyzes Cardiolipin Oxidation

Cardiolipin is an important signature phospholipid of the inner mitochondrial membrane where the lipid is synthesized. It constitutes approximately 20% of the total mitochondrial lipid pool. The dimeric nature and diphosphatidylglycerol structure combined with four acyl chains make cardiolipin a unique mitochondrial lipid, that plays a crucial role in mitochondrial function and, regulation of aggregate structures, triggers apoptosis, and serves as a proton trap for oxidative phosphorylation.

In animal cells, cardiolipin is involved in the process of programmed cell death (apoptosis) through its interaction with the death-inducing protein *Cytc*. *Cytc* is bound to the inner mitochondrial membrane by phospholipids: approximately 15-20% is bound to cardiolipin (Kagan et al., 2004; Schlame et al., 2000). *Cytc* binds to cardiolipin through two sites called the A-site and the C-site. Weak electrostatic interactions occur through the A-site, between negative phosphate groups of cardiolipin and positively charged lysine residues of *Cytc*. The tight and stable conformation through the C-site is achieved by hydrophobic interactions and hydrogen bonding between *Cytc* Asn52 residue and one of the cardiolipin acyl chains that fits into the *Cytc* pocket. Even high ionic strength solutions cannot remove the fraction of hydrophobic membrane-bound *Cytc* (Belikova et al., 2006). However, the interaction between *Cytc* and cardiolipin results in partial unfolding of the enzyme and conformational changes between the heme group and Met-80, making the bond weaker.

Kagan et al. discovered that during apoptosis, the trans-membrane transfer of cardiolipin decreases the affinity of Cyt c for cardiolipin (Kagan et al., 2005). Cardiolipin prompts the peroxidase activity of Cyt c by destabilizing its tertiary structure through hydrophobic interactions. Therefore, the level of free Cyt c is increased in mitochondrial intermembrane space (Iverson and Orrenius, 2004). During the rupture of the mitochondrial outer membrane, free Cyt c can be further released into the cytosol followed by activation of caspases (Kagan et al., 2005). In conclusion, Cyt c plays an essential role in the regulation of apoptotic process (Hüttemann et al., 2011).

1.5.5 Cytochrome c Plays Role in Redox-Coupled Protein Import via Erv1-Mia40

The transport of the mitochondrial nuclear encoded proteins into the mitochondria is performed by TIMs and TOMs, the translocases of the inner and outer membranes (Rehling et al., 2001). The proteins undergo folding and/or assembly into functional proteins by enzymes that convert the apo-form into a holo-form protein. Cyt c is imported into the mitochondrial intermembrane space as apocytochrome c that is synthesized from its nuclear gene. Cyt c heme lyase or holocytochrome- c synthase converts the apo-form of Cyt c to the holo-form by the addition of a heme group (Dumont et al., 1991). Together with the transporters of the outer membrane (TOMs), Erv1, and Mia40 proteins, Cyt c is required in the redox-coupled import of proteins containing twin CX₃C and CX₉C motifs into the mitochondrial intermembrane space. Transported proteins via TOMs go through post-import modifications such as alternative folding. After the Mia40 oxidation, the formation of disulfide bonds occurs between cysteine residues that change the tertiary structure of proteins (Chacinska et al., 2004). This process depends on oxidation by Erv1 which in turn requires the activity of Cyt c (Allen et al., 2005). The electrons derived from the Mia40 import pathway to Cyt c are injected into the ETC (Hüttemann et al., 2011).

1.6 Regulation of Cytochrome *c* and Other Mitochondrial Proteins by Post-Translational Modifications

Considering the multiple roles of mitochondria in energy and ROS production and the central role of *Cytc* in respiration and apoptosis, their activity should be tightly regulated. Regulation of mitochondrial proteins is also required due to the differences in the cellular requirements between tissues and organs. Protein regulation can be achieved by several mechanisms, including gene expression and translation and post-translational modifications (PTMs). In multicellular organisms, cell signaling through PTMs is one of the most crucial regulatory pathways.

1.6.1 Phosphorylation of Cytochrome *c* Regulates Respiration and Apoptosis

Despite numerous studies on *Cytc*, the fact that this mitochondrial protein is subjected to PTMs as a part of cell signaling has remained unknown for a long time. To date, a total of four phosphorylation sites of *Cytc* were unambiguously assigned to Tyr-97, Tyr-48, Thr-28, and Ser-47 by immobilized metal affinity chromatography/nano-liquid chromatography/electrospray ionization mass spectrometry (IMAC/nano-LC/ESI-MS).

For the first time, in 2006, our lab reported that *Cytc* from cow heart is phosphorylated at Tyr-97, one of four tyrosine residues present in the protein (Lee et al., 2006). *Cytc* from cow heart was isolated under conditions that preserve the physiological *in vivo* phosphorylation status. Western analysis with phosphotyrosine-specific antibody revealed a strong signal suggesting that at least one out of the four tyrosine residues was phosphorylated. Only one specific phosphorylation site was assigned by IMAC/nano-LC/ESI-MS to Tyr-97. The phosphorylated Tyr-97 is located on the right side of the molecule. Spectral analysis of phosphorylated Tyr-97

Cytc indicated a shift of characteristic 695 nm absorption band to 687 nm which was reversed after alkaline phosphatase treatment. The interactions between Met-80 and heme iron causes the characteristic 695 nm band; a shift of the band suggests alterations in the catalytic heme crevice and changes in Cytc functions. Furthermore, phosphorylated Cytc at the Tyr-97 residue exhibits enhanced sigmoidal kinetics compared to the SAP-dephosphorylated Cytc and shows inhibition of oxygen consumption with purified COX (Lee et al., 2006).

In 2008, another phosphorylation site of Cytc was identified by our group from cow liver by mass spectrometry on Tyr-48 (Yu et al., 2008). The analysis of oxygen consumption with isolated cow liver COX demonstrated that phosphorylated Tyr-48 Cytc shows a hyperbolic response, similar to unphosphorylated Cytc. The activity of COX was approximately 50% decreased with Tyr-48 phosphorylated Cytc. Structurally, Tyr-48 faces towards the inside of the protein. Additional phosphorylation groups could change the protein structure and alter its function. In a continuation of the above study, Pecina et al. generated a phosphomimetic mutant of Cytc to determine the functional impact of phosphorylated Tyr-48 Cytc *in vitro*. The phosphomimetic substitution of Tyr48Glu mutant Cytc mimics the negative charge of *in vivo* phosphorylation; in addition, WT and Tyr48Phe variants were used as non-phosphorylated controls. The kinetic analysis indicated a hyperbolic response with a 30% decrease of maximal velocity for the phosphomimetic mutant compared to the WT (Pecina et al., 2010). Additionally, compared to the WT control, the phosphomimetic Cytc mutant revealed a reduced midpoint redox potential, by 45mV, and a decreased binding affinity to cardiolipin by 30%. More importantly, this study showed that phosphomimetic Tyr48Gln Cytc was unable to induce downstream caspase-3 activation *in vitro*. The research data suggest that phosphorylation at Tyr-48 residue could function

as an antiapoptotic switch *in vitro* and might have a crucial impact on the understanding of molecular pathways underlying the ability of cancer cells to evade apoptosis (Pecina et al., 2010).

Two other phosphorylation sites, Cyt c Thr-28 and Ser-47 from human skeletal muscle, were discovered by high-throughput phosphoproteomic MS analysis (Zhao et al., 2011). While the functions of Cyt c Ser-47 phosphorylation remain unknown, phosphorylated Thr-28 demonstrated regulatory activity through the ETC in bovine and rat kidney tissue (Mahapatra et al., 2017). Thr-28 is located near the heme crevice. Isolated Cyt c from bovine and rat kidney tissue is phosphorylated on Thr-28. Phosphorylated Cyt c *in vivo* and phosphomimetic T28E mutant cause inhibition of respiration with purified COX.

Intact cells expressing T28E phosphomimetic Cyt c showed a 60% decrease in respiration activity, supporting the *in vitro* results with purified COX. Additionally, mitochondrial membrane potential and ROS levels in the intact Cyt c knock-out cells showed reduced levels compared with WT, suggesting that the phosphomimetic mutant can protect cells. Furthermore, compared to previous studies on Tyr-48 phosphorylated Cyt c , phosphorylated Thr-28 and WT were able to trigger caspase-3 activation, suggesting that Thr-28 does not influence the apoptotic function of Cyt c . Phosphorylation, or in other words, the introduction of a negative charge at Thr-28 residue, improved protein stability and resistance to degradation in the presence of excess H₂O₂ compared to WT control. Considering that the reduction rate of oxidized Thr-28 mutant was twice the rate of WT, it was proposed that Thr-28 phosphorylated Cyt c can function as an electron acceptor and ROS scavenger. Interestingly, the peroxidase activity of the phosphomimetic mutant was much lower compared to WT. The results of this study suggest that the regulation of ETC flux through Cyt c phosphorylation prevents hyperpolarization of mitochondrial membrane potential to prevent the generation of ROS.

1.6.2 Methylation of Lysine Residues of Cytochrome *c*

It has long been known that Lysine, Arginine, Histidine, and dicarboxylic amino acids can accept an additional methyl group. In the histones, the ϵ -NH₂ group of Lysine residues can be mono-, di- or tri-methylated. Protein methylation regulates many biological functions, such as gene regulation and signal transduction (Paik et al., 2007). It was reported that a lysine ϵ -NH₂ group of *Cytc* is methylated *in vivo* (Pahlich et al., 2006). Methylation of *Cytc* increases protein stability *in vivo* and supports resistance to proteolytic digestion *in vitro* (Paik et al., 2007).

It has been shown in *Saccharomyces cerevisiae* and plants that *Cytc* expressed from the *CYCI* gene is immediately trimethylated by the *Cytc* methyltransferase Ctm1p at an evolutionarily conserved Lys-78 residue (usually referred to Lys-72 by homology to vertebrates) (Holzschu et al., 1987; Paik et al., 1989). Although *Cytc* methylation does not usually occur in higher organisms, it is an essential PTM in yeast. Trimethylation supports its transport into the mitochondrial inner membrane space (Park et al., 1987). *Cytc* methyltransferase Ctm1p is regulated by Cyc1p, and can carry electrons between complex III and complex IV in the ETC. Cyc1p also participates in the response to oxidative stress (Kwon et al., 2003; Volkov et al., 2011) and protein import into the mitochondrial intermembrane space in yeast (Dabir et al., 2007; Hell, 2008; Herrmann and Riemer, 2012). Methylation of Cyc1p could change its geometry, *PI*, or conformation (Brems and Stellwagen, 1981; Kim et al., 1980; Pollock et al., 1998). Additionally, a structural analysis demonstrated that trimethyllysine 78 is essentially positioned across the heme crevice loop, playing a crucial role in opening the crevice (Cherney et al., 2013). Later, in 2015, Winter et al. demonstrated that methylation of Cyc1p increases its interactions with Erv1p and Cyc3p. This supports the addition of the heme group to Cyc1p, hence trapping it in the mitochondrial intermembrane space (Winter et al., 2015).

Polastro et al. have shown that in *Ascomycetes*, methylation at Cyt_c Lysine72 residue maintains the binding of the hemoprotein to mitochondria. They concluded that methylation of the protein is essential for the physiological processes, including electron transport through the ETC (Polastro et al., 1978). Later, in 1980, Farooqui et al. reported that Cyt_c from fungi and plants is methylated by S-adenosylmethionine: cytochrome c-lysine N-methyltransferase. The group demonstrated that methylation of Cyt_c at the lysine residue protects the protein against the intracellular proteolytic enzyme attack *in vivo* (Farooqui et al., 1981). Furthermore, the methylation at Lys-72 Cyt_c showed the pro-apoptotic activity of the hemeprotein (Kluck et al., 2000).

1.6.3 Mitochondrial Lysine Acetylation

Modifications of the lysine amino acid are crucial for mitochondrial physiology, owing to the localization of the specific metabolites in the mitochondrial matrix. Under physiological conditions, modification on the ϵ -amino group of lysine residues show a remarkable chemical diversity with about twenty modifications (Figure 4) (Hosp et al., 2017). Lysine acetylation is the most frequent PTM within mitochondria. In 2006, Kim et al. identified and analyzed 388 acetylation sites on 195 proteins from isolated mouse liver mitochondria and HeLa cells (Kim et al., 2006). Recent studies have confirmed that the mitochondrial proteome is acetylated; more than 60% of the proteins have one or more acetylation sites (Anderson and Hirschey, 2012; Hebert et al., 2013; Konig et al., 2014; Smith-Hammond et al., 2014). The TCA cycle, ETC, and ATP synthase are conserved targets for lysine acetylation in various species. It has been reported that isocitrate dehydrogenase 2 (IDH2), malate dehydrogenase (MDH), and succinate dehydrogenase (SDH) are found to be acetylated (Lin et al., 2014). Furthermore, skeletal muscle, heart, liver, and

directly affect mitochondrial functions and lead to different human illnesses, such as heart diseases, cancer, and neurodegenerative disorders.

1.7.1 Mitochondrial Protein Hyperacetylation in the Failing Heart

The energy stores of cardiomyocytes are limited; therefore, heart tissue requires a high level of ATP to maintain its contractive function. Mitochondrial dysfunction and energy depletion are linked to the impaired myocardial energetics, trigger oxidative stress and lead to the development of heart failure (HF) (Horton et al., 2016). Recent studies indicate that lysine acetylation of mitochondrial proteins contributes to the sensitivity of the heart to stress and cell death (Lee and Tian, 2015). In 2012, Grillon et al. identified a non-histone protein acetylation in the failing heart for the first time. In spontaneously hypertensive HF prone and Dahl salt-sensitive animal models, 66 and 41 acetylated proteins were found respectively (Grillon et al., 2012). This suggests a reduced level of SIRT3 in the failing heart. SIRT3, mitochondrial NAD-dependent deacetylase, modulates cardiomyocyte resistance and survival during oxidative stress. Later, in 2013, it was shown that the level of SIRT3 is dramatically decreased in the failing heart from rat (Chen et al., 2013) and that the progression of the disease was linked to the increased level of mitochondrial protein acetylation in the murine model of diabetic cardiomyopathy (Vadvalkar et al., 2013).

Additionally, increased acetyl-CoA levels that were found in the human failing heart can drive acetylation of mitochondrial proteins, which in turn might trigger enzymatic dysfunction (Baeza et al., 2016). Based on these results, Horton et al. considered that during the progression of heart failure, aggregation of fuel oxidation pathway metabolic intermediates trigger PTMs of mitochondrial proteins. They showed that 82 out of 383 mitochondrial proteins were acetylated at

the 244 acetylated lysine sites seen in the cardiac hypertrophy and failing mouse heart. Progressive mitochondrial protein lysine acetylation take place in OXPHOS pathways, since most of the identified acetylated proteins are involved in the ETC, TCA cycle, and β -oxidation pathways (Horton et al., 2016). The authors also emphasized that succinate dehydrogenase A (SDHA), the only enzyme that participates in both the TCA cycle and the ETC, is hyperacetylated at several lysine residues in human and mouse samples. The mutagenesis study of acetyl-mimetic K179Q mutant reveals reduced catalytic function and lowered complex II-driven respiration (Horton et al., 2016).

The collective results suggest that extensive mitochondrial protein lysine acetylation, driven by the increased level of acetyl-CoA and reduced NAD^+ levels, leads to decreased oxidative flux, depletion of ATP, and hence to the development of HF.

1.7.2 Impact of Acetylation on the Neurodegenerative Diseases

To date, Alzheimer disease (AD) is the most prevalent neurodegenerative disorder which is characterized by the intracellular accumulation of hyper-phosphorylated *tau* protein in neurons. Senile plaques in the brain are composed of β -amyloid ($\text{A}\beta$) aggregates, which can cause neuronal death. Most proteins that are involved in the progression of AD are targets of SIRT1 and regulated by lysine acetylation (Michan, 2013). Cognitive defects *in vivo* are usually the result of acetylation of human *tau* protein at Lys-174, Lys-274, and Lys-280 (Cohen et al., 2011). Additionally, the acetyl mimetic, *tau* K280Q, increased neurotoxicity in a *Drosophila melanogaster* model *in vivo* (Gorsky et al., 2016).

Mitochondrial acetylation is also observed in Parkinson's (PD) and Huntington's diseases (HD). In animal models of PD, acetylation triggers mitochondrial autophagy that is regulated by

PINK1 and Parkin proteins (Auburger et al., 2014). HD, a trinucleotide cytosine-adenine-guanine (CAG) repeat disorder, causes glutamine expansion (PolyQ). The Huntington protein (HTT) that is largely expressed in the brain regulates neurotransmission. Misfolded HTT causes protein aberration and the formation of aggregates, accumulation of which leads to the neuronal death. Michan et al. demonstrated that in *Drosophila melanogaster*, the mitochondrial global acetylation level could be reduced by the interactions between the polyQ stretches and the acetyltransferase domain of proteins (Michan, 2013). In mouse brains, acetylation at the K444 residue of mutant HTT stimulates autophagy-mediated protein degradation and decreases neurotoxicity (Jeong et al., 2009).

1.7.3 Acetylation of Lysine Residues in Cancer Metabolism

PTMs are most commonly dysregulated in different types of cancer, including prostate cancer. In prostate cancer androgen signaling plays an essential role in triggering cancer cell proliferation (Carver, 2014). Cancer cells use mitochondria as signaling organelles, and mitochondria are required for cancer bioenergetics and biosynthesis of macromolecules (Weinberg and Chandel, 2015). Protein acetylation of intermediary metabolism could affect survival of cancer cells both, positively or negatively (Choudhary et al., 2009; Guan and Xiong, 2011; Kim et al., 2006). Acetylation of pyruvate dehydrogenase phosphatase 1 (PDP1) at residue K202 and pyruvate dehydrogenase (lipoamide) alpha1 at residue K321 leads to enzymatic dysfunction and disassembly of the pyruvate dehydrogenase complex, promoting cancer cells to depend on glycolysis (Fan et al., 2014). Recent studies indicate that acetylation of proteins participating in glycolysis may alter cancer cell growth (Lv et al., 2011). Lysine acetylation of PKM2 inhibits enzyme activity and causes an aggregation of glycolytic intermediates to maintain tumor growth.

Acetylation of lactate dehydrogenase (LDH) at residue K5 has the opposite effect. Destabilization and reduced activity of acetylated enzymes leads to the depletion of the NAD⁺ pool in glycolysis. Additionally, lysosomal protein degradation and chaperone-mediated autophagy are triggered by interaction between acetylated LDH and the HSC70 chaperone protein. Deacetylation of LDH by SIRT2 supports the activation of the enzyme as well as pancreatic tumor growth in both *in vitro* and *in vivo* studies (Zhao et al., 2013). Another study on pancreatic cancer indicates that acetylation of mitochondrial glutamate oxaloacetate transaminase at K159, K185, and K404 residues enhances the interactions with malate dehydrogenase. These interactions elevate the activity of the malate-aspartate shuttle to increase ATP production for the tumor growth (Yang et al., 2015). In addition to the pancreatic studies, lung cancer research reported that the acetyl-mimetic mutant Lys100Gln of phosphoglycerate mutase 2 (PGAM2) suppresses cell proliferation and cancer growth in A549 lung cancer cell line and tumor xenografts *in vitro* and *in vivo*.

To maintain cell proliferation and tumor progression, cancer cells utilize increased lipid biosynthesis. Cytosolic acetyl-CoA required for lipogenesis is produced by the ATP-citrate lyase (Lin et al., 2013). Acetylation of the enzyme at K540, K546, and K554 stabilizes the protein and increases lipid synthesis. Therefore, acetylation at specific residues can enhance cell proliferation and cancer growth *in vivo*.

1.8 Prostate Cancer

Prostate cancer is one of the most common types of cancer in men and the second leading cause of cancer death among men in America. The American Cancer Society estimated that more than 220,800 men were newly diagnosed with this pathology in 2015, more than 27,540 men died

from the disease, and approximately 1 man in 7 will be diagnosed with prostate cancer during his lifetime.

Prostate cancer, or carcinoma, is a disease of the prostate gland of the male reproductive system (Figure 5). A prostate is a small walnut-shaped exocrine gland which secretes a slightly alkaline seminal fluid that nourishes and transports sperm. Carcinoma begins with small alterations in the shape, size, and uncontrollable growth of the prostate gland cells, which are called prostatic intraepithelial neoplasia (PIN). Whereas most prostate cancers usually grow slowly, some types can be aggressive and grow relatively quickly. Additionally, these more aggressive types of prostate cancer might spread to other parts of the body, particularly the bones and lymph nodes. Almost all prostate cancers are adenocarcinomas; however, other rare types exist including sarcomas, small cell carcinomas, neuroendocrine tumors, and transitional cell carcinomas.

Despite more than 70 years of cancer research, a full understanding of cancer cause has not yet been achieved. The past and current studies indicate some risk factors of prostate cancer, including age and a family history of the disease. The disease typically occurs in men over the age of 50 and having prostate cancer one's family history increases the risk two to threefold for the individual. Other factors that might be involved in prostate cancer development are a diet high in processed and red meat, milk products, and low in certain vegetables.

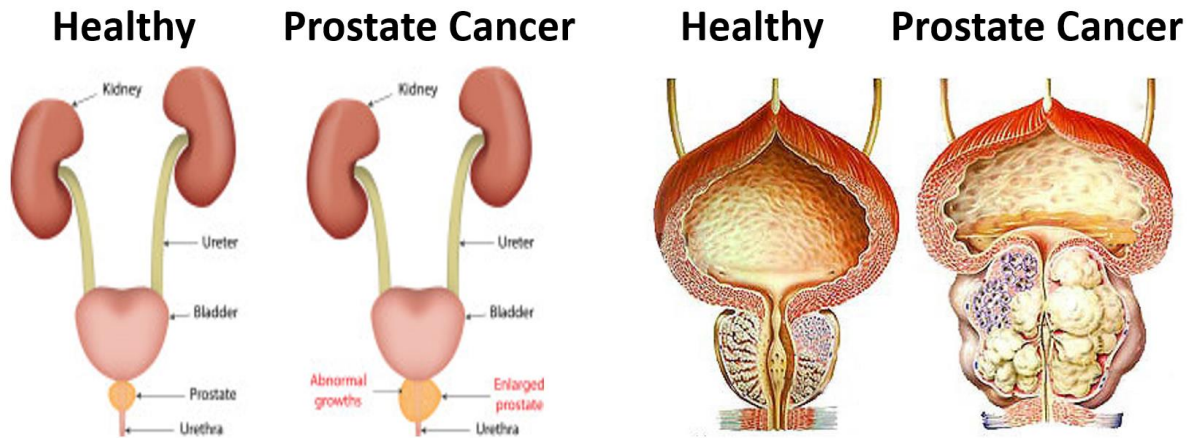


Figure 5. Healthy prostate and prostate cancer. Prostate cancer is characterized by small alterations in the shape, size, and uncontrollable growth of the prostate gland cells. The picture is taken from Urology associates. <https://denverurology.com/male-urology/prostate-cancer/>

Prostate cancer is diagnosed by biopsy, however, one of the most problematic aspects of this pathology is that there are no symptoms in the early stages; therefore, it is difficult to diagnose it in time. Treatment modalities for prostate cancer range from surgery and radiation to chemotherapy. If left untreated, prostate cancer cells are able to spread by breaking away from a prostate tumor and moving through blood or lymph vessels. They may attach to other tissues, producing secondary tumors in a process known as metastasis.

1.9 Metabolic Shift in Cancer: the Warburg Effect

As compared to a healthy cell, the progression of cancer follows a metabolic change from depending primarily on mitochondrial respiration to depending primarily on glycolysis. This switch is known as the Warburg effect, or aerobic glycolysis (Warburg, 1956; Warburg et al., 1924).

In the 1920's a German biochemist and Nobel laureate, Otto Heinrich Warburg was characterizing the growth of rat hepatocarcinoma cells *in vitro* and observed that even in the presence of oxygen, most tumor cells exhibited an increased rate of glycolysis. He discovered that unlike most normal tissues, tumor cells convert the majority of glucose carbon to lactate in the cytosol (Figure 6), even in oxygen-rich conditions, hence the term is 'aerobic glycolysis'. Warburg attributed this change to mitochondrial defects that he proposed inhibited their ability to effectively oxidize glucose carbon to CO₂. He hypothesized that this altered metabolism is specific to cancer cells and it unleashes a potential etiology of cancer origins. However, newer research has shown that mitochondria are functional in most cancer cells; therefore, other mechanisms, such as metabolic reprogramming, may explain the reduced aerobic activity found in cancer (Ward and Thompson, 2012).

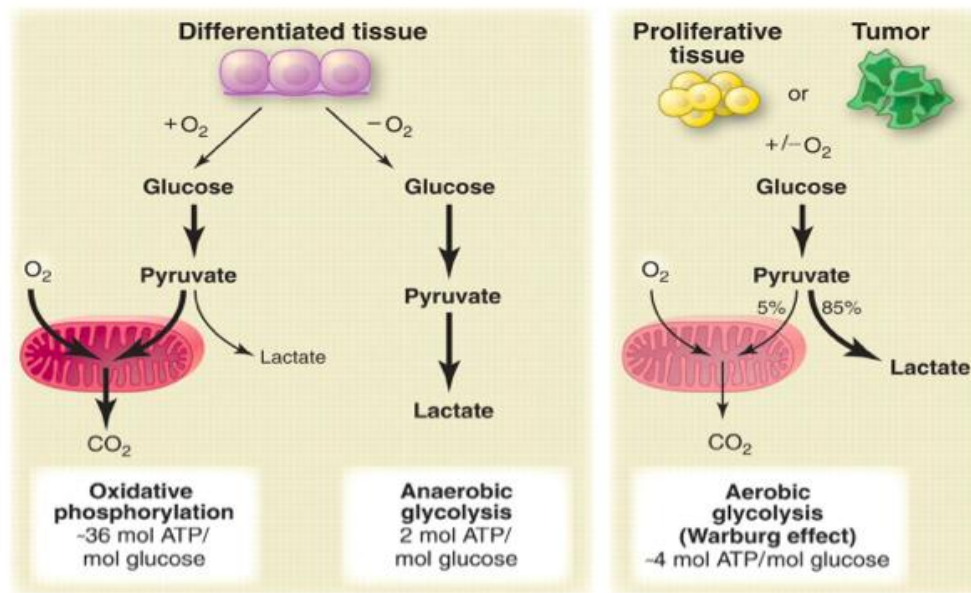


Figure 6. Metabolic shift in cancer cells - the Warburg effect. Comparison of Glycolysis Between a Normal Tissue (total 38 ATP) and Tumour/Proliferated Tissue (total 4 ATP). The picture is taken from (Vander Heiden et al., 2009).

In healthy, non-malignant cells, in the presence of oxygen, one glucose molecule is converted into pyruvate in the cytosol, then transported to the mitochondria where it is metabolized through the TCA cycle and finally the ETC, yielding 36 molecules of ATP. Warburg observed that cancer cells undergoing aerobic glycolysis and convert approximately 85% of glucose to lactate in the cytosol with limited ATP production (one molecule of glucose yields 2 molecules of ATP) but increased macromolecule production. This leads to a biosynthetic metabolic shift towards the pentose phosphate pathway (PPP) for the production of NADPH and ribose-5-phosphate to increase nucleotide synthesis. This is essential for the high proliferation rate seen in cancer cells.

CHAPTER 2

THE EFFECT OF ACETYLATION OF CYTOCHROME C ON ITS FUNCTIONS IN CANCER

2.1 Background and Purpose of Study

Cytochrome *c* (Cyt*c*) is a small multifunctional globular protein with a covalently attached heme group. Cyt*c* is involved in cellular life and death decisions. The protein is located in the mitochondrial intermembrane space, where it functions as an electron carrier between *bc*₁ complex and COX in the ETC, playing an important role in the generation of cellular ATP. Cyt*c* knockout mice die around midgestation, when a metabolic switch occurs from the glycolytic pathway to aerobic energy production. Additionally, Cyt*c* plays another crucial role in type II apoptosis, which involves the release of Cyt*c* from the mitochondria into the cytosol, where it activates downstream caspases after the formation of the apoptosome. We propose that all Cyt*c* functions are regulated through cell signaling pathways. The three major functions of Cyt*c*, (mitochondrial respiration, apoptosis, and ROS generation or scavenging) are all altered in cancer, leading to Warburg metabolism and evasion of apoptosis (Hüttemann et al., 2014).

The importance of Cyt*c* has long been recognized; however, the fact that it can be posttranslationally modified has remained unknown until recently. In the Hüttemann lab, it was shown that Cyt*c* is posttranslationally modified by phosphorylation of tyrosine residues in healthy tissues on two distinct tyrosine residues *in vivo*, Tyr-97 and Tyr-48 in heart and liver tissue, respectively (Lee et al., 2006; Yu et al., 2008). Importantly, our preliminary data indicates that human Cyt*c* is acetylated on lysine 53 (Lys-53) in castrate-resistant and castrate-sensitive prostate tumor xenografts. This is the first time that Cyt*c* acetylation has been identified in mammals.

The results of mass spectrometry unambiguously assigned acetylation site on Lys-53 in both castrate-resistant and - sensitive tumors, therefore it has been proposed that the Cyt c acetylation state changes from a “healthy” to a “cancer” state (Figure 7) in prostate cancer, where the Warburg effect causes the inhibition of the mitochondria respiration. The other hypothesis was that the acetylation of Cyt c prevents the involvement of Cyt c in cell death in cancer.

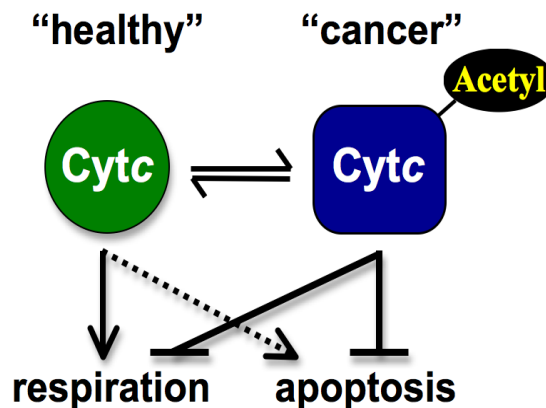


Figure 7. Model of cytochrome c regulation. Under healthy conditions (left) Cyt c allows efficient energy production through the mitochondrial pathway. Cancer signaling (right) leads to a change in its acetylation state causing an inhibition of respiration (“Warburg effect”), and it also renders Cyt c incapable to trigger apoptosis allowing cancer cells to evade apoptosis.

In vitro studies have shown that phosphorylation of Tyr-48 could operate as a toggle, fully inhibiting the capability of Cyt c to trigger apoptosis (Pecina et al., 2010). Similar to phosphorylation, Lys acetylation results in a net increase of a negative charge, as a positive charge is lost upon acetylation. The net charge changes plus the position of Lys-53 which is located on the same domain of Cyt c as Tyr-48, support our hypothesis that acetylation may also act as a switch for apoptosis in cancer cells. The previous results indicate that cellular respiration and apoptosis

are regulated by cell signaling via *Cytc* posttranslational modifications, and suggest a regulation of *Cytc* in cancer (Carver, 2014; Hüttemann et al., 2014).

Considering the importance of *Cytc* in both respiration and apoptosis, it is still unknown how these functions are regulated in cancer. Therefore, the main goal of this study is to understand the regulation of mitochondrial respiration and apoptosis in cancer via regulation of *Cytc*. In order to test the hypothesis that acetylation of *Cytc* leads to inhibition of respiration and apoptosis, the acetyl-mimetic and control *Cytc* will be used as a model system to study *Cytc* function *in vitro*.

2.2 Materials and Methods

2.2.1. Generation of Cytochrome *c* Variants

The bacterial expression plasmid pLW01 (gift from Dr. Lucy Waskell, University of Michigan), was used to generate *Cytc* variants and to overexpress them in the bacterial prokaryotic system. Bacteria do not have *Cytc* heme lyase (CYC3) (holo cytochrome *c* synthase), an enzyme catalyzing the attachment of heme to apo-cytochrome *c*, the pLW01 plasmid contains the cDNA encoding CYC3 (Figure 8). *Cytc* mutants were expressed in *Cytc* double knock-out mouse lung fibroblasts (Vempati et al., 2007) using the mammalian expression plasmid, pBABE-puro (Catalog # 1764, Addgene, Cambridge, MA) (Figure 9).

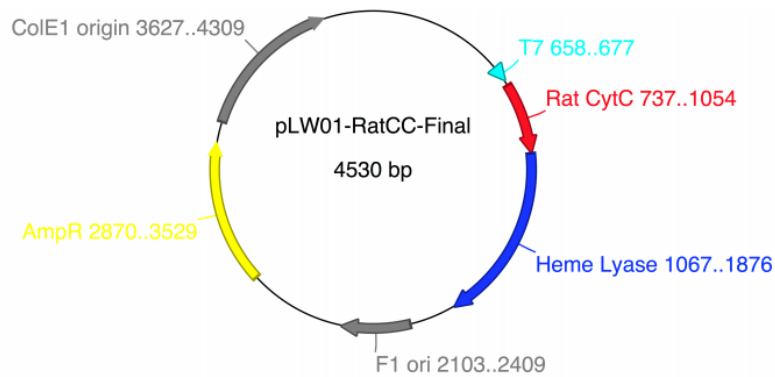


Figure 8. pLW01 expression vector. The bacterial expression plasmid pLW01 contains the cDNA encoding *Cytc* heme lyase (CYC3), an enzyme that covalently links the heme group to the apoprotein of *Cytc*.

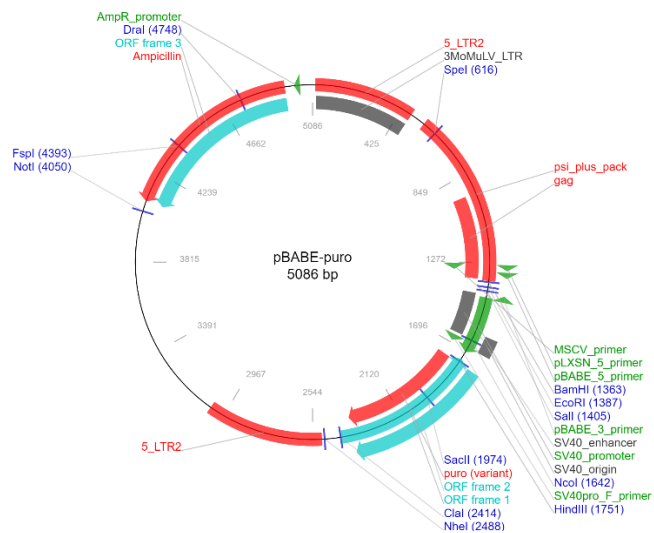


Figure 9. pBABE-puro expression vector. Mammalian expression plasmid containing the bacterial origin of replication, ampicillin-resistance gene, and puromycin-resistance gene for selection stable cell lines. The picture is taken from Addgene, Cambridge, MA, <https://www.addgene.org/1764/>

Site-directed mutagenesis was applied to produce three *Cytc* variants. The cDNA of non-acetylated wild type *Cytc* contains a lysine residue at position 53 which was mutated to the acetylmimetic glutamine, a non-acetylated arginine that carries a positive charge, and to the nonpolar isoleucine as an additional control. The QuickChange II Site-Directed Mutagenesis Kit (Catalog # 200523, Agilent Technology, CA) was used to introduce the desired mutations and to clone the mutated cDNA into pLWO1 and pBABE-puro expression vectors. The quick manufacturer's protocol (Figure 10) allows generating mutations with the efficiency higher than 80%.

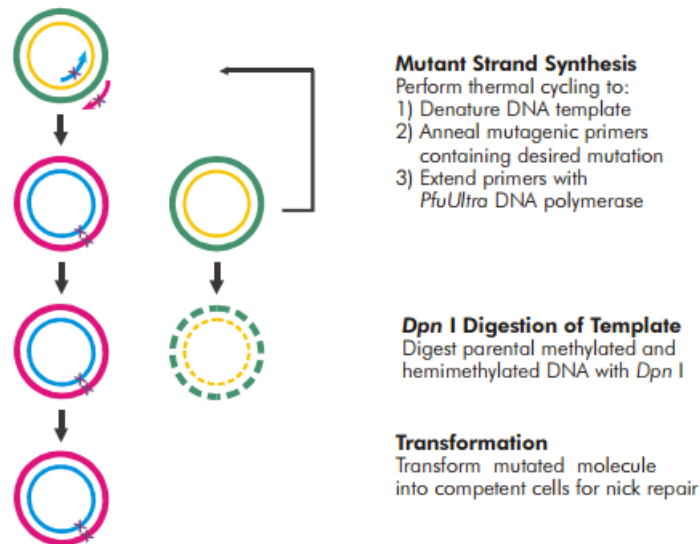


Figure 10. Overview of the QuickChange II site-directed mutagenesis method. The QuickChange II Site-Directed Mutagenesis Kit allows introducing a site-specific mutation in a double-stranded plasmid. The kit does not require unique restriction sites and multiple transformations. The picture is taken from Agilent Technology, CA <http://www.genomics.agilent.com/article.jsp?pageId=384>

For each *Cytc* variant, two synthetic oligonucleotide primers complementary to the opposite strand of the vectors were designed for use in thermocycling PCR (Table 2). During PCR, primer extension by PfuUltra high-fidelity DNA polymerase creates a mutated plasmid. The mutated plasmid is then digested for one hour at 37°C with Dpn I, a specific endonuclease which digests the parental methylated DNA, making it possible to isolate plasmids with the introduced mutations. The mutant plasmids were then transformed into the XL1-Blue competent cells and were plated on the agar plates with 100 µg/mL ampicillin. Plates were incubated overnight at 37°C. Next day, colonies were transferred to the cell-culture tubes with 5 mL of LB medium with 100 µg/mL ampicillin and were grown overnight at 37 °C under constant shaking. All plasmids from overnight culture were purified using the QIAprep Spin Miniprep Kit (Catalog # 27106, Qiagen, Valencia, CA) following the manufacturer's protocol. NanoDrop 1000 Spectrophotometer (Thermo Fisher Scientific, Waltham, MA) was used to quantify and assess the purity of DNA. The desired *Cytc* constructs were confirmed by sequencing.

Table 2. Designed primers for the QuickChange II site-directed mutagenesis protocol

Name	Primer's Sequences	Tm (°C)
Lys53Gln, Forward primer	5' CTT ACA CAG ATG CCA ACC <u>AGA</u> ACA AAG GTA TCA CC 3'	62.8
Lys53Gln, Reverse primer	5' GGT GAT ACC TTT GTT <u>CTG</u> GTT GGC ATC TGT GTA AG 3'	62.8
Lys53Arg, Forward primer	5' CTT ACA CAG ATG CCA ACA <u>GGA</u> ACA AAG GTA TCA CC 3'	62.8

Lys53Arg, Reverse primer	5' GGT GAT ACC TTT GTT <u>CCT</u> GTT GGC ATC TGT GTA AG 3'	62.8
Lys53Ile, Forward primer	5' CTT ACA CAG ATG CCA ACA <u>TTA</u> ACA AAG GTA TCA CCT G 3'	61.4
Lys53Ile, Reverse primer	5' CAG GTG ATA CCT TTG <u>TTA</u> <u>ATG</u> TTG GCA TCT GTG TAA G 3'	61.4

2.2.2. Bacterial Overexpression of Cytochrome *c* Variants

Sequence-confirmed PLWO1 constructs were used to transform competent C41(DE3) *E.coli* cells (Catalog # 60442-1, Lucigen, Middleton, WI) for protein overexpression and purification, using the heat shock method. Competent C41(DE3) cells were thawed on ice. DNA at a concentration of 50 ng was added to the competent cells. Culture tubes with a mixture containing cells and DNA were incubated on ice for 30 minutes and then placed in a 42°C water bath for 45 seconds (heat shock), followed by incubation on ice for 2 min. 950 µL of room temperature LB medium was added to the cells, and culture tubes were placed in a shaking incubator at 250 rpm for 1 hour at 37 °C. 200 µL of the transformation was plated on LB-agar plates containing 100 µg/mL ampicillin and incubated overnight at 37°C. Selected clones were inoculated into 10 mL of LB medium with 100 µg/mL ampicillin and were grown overnight at 37 °C under constant shaking. The overnight culture was added into three flasks with 1L of TB medium (Difco, BD, Franklin Lakes, NJ) and 100 µg/mL of carbenicillin. The culture was grown until an OD₆₀₀ of 1-1.5 was reached. At this point, 100 mM isopropyl β-D-1-thiogalactopyranoside (IPTG) was added to induce the expression of Cyt*c*. The induced cultures were incubated for 6 h and, every 2 h, 1mL of culture was collected to check the expression by Western blotting. The

bacterial cells were pelleted by centrifugation at 4500 rpm, for 40 min at 4°C. The cell pellets were instantly frozen and stored at - 80 °C.

2.2.3. Western Blotting Analyses of the Overexpressed Cytochrome *c*

Western blotting analyses were performed to analyze the bacterial overexpression of Cyt*c*, with a 1:1000 dilution of mouse Anti-Cytochrome *c* primary antibodies (BD Pharmingen), followed by a 1:5000 dilution of Anti-mouse IgG, horseradish secondary antibody (GE Healthcare). Sigma cytochrome *c* was used as a control. The overexpression of Cyt*c* was checked after 0, 2, 4, and 6 hours after IPTG induction. One mL of culture was collected at each time point and centrifuged for 5 min at max speed. The bacterial cell pellets were resuspended in lysis buffer (20 mM phosphate buffer, pH 7.4), supplemented with a protease inhibitor mixture (P8340) as recommended by the manufacturer. The concentration of cell lysate was determined by the DC Protein Assay (Catalog # 5000111, Bio-Rad, Hercules, CA) following the manufacturer's protocol. Twenty µg of protein lysate were denatured at 95°C for 5 min after mixing with 4X loading buffer. The protein samples were separated using 12% SDS-PAGE and then transferred to PVDF membranes (0,2 µm, Bio-Rad, Hercules, CA) using a semi-dry apparatus (Bio-Rad, Hercules, CA). The membrane was blocked with 5% non-fat dry milk for 1 hour, and then incubated with the primary antibody under shaking overnight at 4°C, followed by incubation with the respective secondary antibody for 2 h at room temperature. Each incubation was followed by washing the membrane with 1x TBS-T 6 times for 10 min. The signal was detected with HyGLO chemiluminescent HRP detection reagent (Catalog # E2500, Denville Scientific Inc, NJ) following the manufacturer's protocol.

2.2.4. Purification of Cytochrome *c* Variants

The bacterial cell pellets were thawed and resuspended in lysis buffer (20 mM phosphate buffer, pH 7.4), supplemented with a protease inhibitor mixture (P8340) as recommended by the manufacturer. For each 10 g of pellet, 100 mL of lysis buffer were used. The cells afterward were lysed by a French Pressure Cell Press (AMINCO, American Instrument Co.). To remove cell debris, the cell lysates were centrifugated for 45 min at 15,000 rpm. The supernatant was adjusted to pH 7.5 and diluted with ddH₂O until a conductivity of 4 mS/cm was reached and matched with the DE52 anion-exchange column (Whatman, Piscataway, NJ). Adjusted supernatant was applied to the equilibrated DE column. Most of the bacterial proteins were bound to the column and Cyt*c* was collected within the flow-through. The collected solution was adjusted to pH 6.5 and conductivity was increased by addition of KH₂PO₄ buffer until it reached 6 mS/cm and matched with the CM52 cellulose cation-exchange column (Whatman, Piscataway, NJ). The adjusted flow-through was applied to the previously equilibrated CM column with 40 mM phosphate buffer, pH 6.5, allowing the positively charged Cyt*c* to bind to the CM column. After washing the CM column, the bound Cyt*c* was eluted with high salt buffer (0.5 M NaCl in 40 mM phosphate buffer, pH 6.5). Cyt*c* fractions were desalted and concentrated by centrifugation using Amicon Ultra-15 3k units (Catalog # UFC901008, Millipore, Billerica, MA). Cyt*c* was aliquoted and stored in -80°C. The workflow of the expression and purification of Cyt*c* variants is presented in Figure 11.

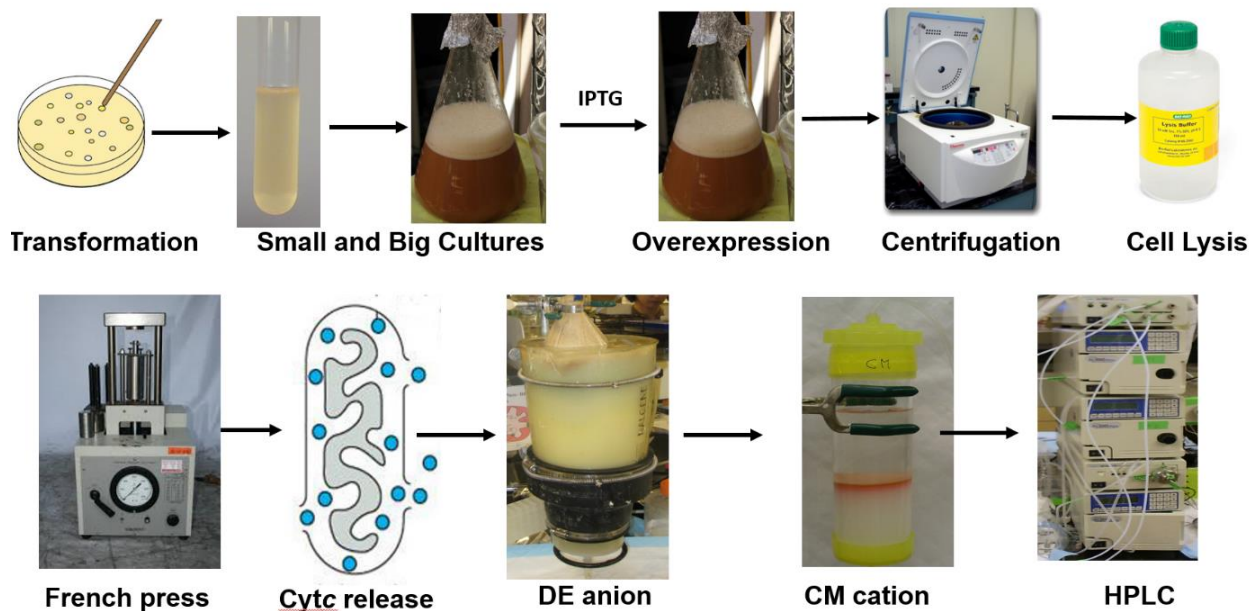


Figure 11. Expression and purification of cytochrome *c* variants. Flowchart of recombinant protein expression and purification via two steps ion exchange chromatography.

2.2.5. Analysis of Cytochrome *c* Absorption Spectra

100 μM of Cyt c mutants were oxidized with a few granules of $\text{K}_3\text{Fe}(\text{CN})_6$ and desalted with NAP-5 columns (Catalog # 17-0853-02, GE Healthcare, Piscataway, NJ). Absorption spectra were recorded on a Jasco V-570 double beam spectrophotometer (2 nm bandwidth, 200 nm/min scanning speed). Reduced Cyt c was obtained by adding a few granules of sodium dithionite, removing reductant via NAP-5 columns, and acquiring spectra as described above (Pecina et al., 2010).

2.2.6. Determination of the Concentration of Cytochrome *c* Variants

Purified Cyt c variants (WT, Lys53Arg, Lys53Gln, and Lys53Ile) were reduced with a few granules of sodium dithionite and desalted with NAP-5 columns (Catalog # 17-0853-02, GE

Healthcare, Piscataway, NJ). Absorption spectra at 550 nm for each mutant were recorded on a Jasco V-570 double beam spectrophotometer (2 nm bandwidth, 200 nm/min scanning speed) using a 0.1-mm path length quartz cuvette. Afterwards, Cyt c mutants were oxidized with a few granules of $K_3Fe(CN)_6$ and desalted with NAP-5 columns. The acquisition of absorption spectra at 550 nm were recorded as described above. The concentration of Cyt c variants were defined by differential spectra at 550 nm by subtracting the oxidized form from the reduced form and calculated via Cyt c (mM) = $Ab_{550_{red}} - Ab_{550_{ox}} / 19.6 \times \text{dilution factor}$.

2.2.7. Mass Spectrometry of Castrate-Resistant and Castrate-Sensitive Prostate Tumor Xenografts to Detect Site-Specific Acetylation

Castrate-resistant (PC3) and castrate-sensitive (VCaP) prostate cancer cells were implanted into SCID mice at the Animal Model and Therapeutics Evaluation Core under Dr. Polin. Tumors were harvested and Cyt c was purified by immunoprecipitation and analyzed by mass spectrometry. Peptides were injected into the mass spectrometer (LTQ Orbitrap-Velos, Thermo Scientific, Waltham, MA) after electrospray ionization. MS/MS spectra were obtained in positive ion mode, assigned to peptide sequences from the UniProt protein database, searched with the MASCOT algorithm for PTMs, and manually verified.

2.2.8. Caspase-3 Activity Induction by Cytochrome c Variants

The ability of purified Cytochrome c variants to induce caspase-3 activation was assayed *in vitro* with cytoplasmic extracts prepared from cultured HeLa cells, previously described (Slee et al., 1999). After trypsinization, cells from 8 x 75 cm² flasks were pelleted by 4°C centrifugation and washed twice with 1x PBS, followed by washing with ice-cold cell extraction buffer (CEB:

20 mM HEPES, pH 7.5, 10 mM KCl, 1.5 mM MgCl₂, 1 mM EDTA, 1mM EGTA, 1 mM dithiothreitol, 100 μM PMSF). The pellet was gently resuspended in two volumes of CEB and transferred to an ice-cold Dounce homogenizer. Cells were disrupted by 20 strokes with a B-type glass pestle after 15 min of swelling on ice. Cell breakage was confirmed using a microscope. The lysates were transferred to microcentrifuge tubes and centrifuged at 15,000g for 15 min at 4°C to remove nuclei and debris. The protein concentration of the supernatant, containing cytosolic fraction, was determined by DC Protein Assay (Catalog # 5000111, Bio-Rad, Hercules, CA). The EnzChek Caspase-3 Assay Kit # 2 (Catalog # E13184, Invitrogen, Carlsbad, CA) with the rhodamine 110-linked DEVD tetrapeptide, an artificial substrate for caspase-3 that fluoresces upon caspase-3 cleavage, was used to measure Caspase-3 activity. Cytosolic extracts at a concentration of 2 mg/mL were incubated with 15 μg/mL of Cyt c variants for 2.5 h at 37 °C. Aliquots of 10 μL of activated extracts after incubation were assayed for caspase-3 activity in triplicates. The same aliquots were used for the triplicates containing a caspase-3 inhibitor in parallel. A Fluoroskan Ascent FL plate reader (Labsystems, Thermo Scientific, Waltham, MA) was used to detect fluorescence from the cleavage of the artificial caspase-3 substrate over 3 h in 30-min intervals, using excitation filter 485 nm/14 nm bandwidth, and emission filter 527 nm/bandwidth 10 nm. The amount of cleaved caspase-3 substrate was calculated from the rhodamine 110 calibration curve. Data values are expressed in % fluorescence of WT. The signal from caspase-3 inhibitor wells was subtracted from the results, as a background (Pecina et al., 2010).

2.2.9. Cytochrome c Oxidase Activity Measurements

Previously isolated regulatory-competent bovine liver COX was used for this experiment (Lee et al., 2009). A COX aliquot was diluted to the final concentration of 3 μM in the presence

of a 40-fold molar excess of cardiolipin and 0.1 mM ATP in COX measuring buffer (10 mM K-HEPES (pH 7.4), 40 mM KCl, 2 mM EGTA, 10 mM KF, 1% Tween 20). To remove cholate bound to COX during enzyme purification, the diluted aliquot of COX was dialyzed overnight at 4°C. Respiration of COX (150 nM) was analyzed in a closed chamber equipped with a micro-Clark-type oxygen electrode (Oxygraph system, Hansatech, Pentney, UK) (Figure 12) at 25°C in 220 µL of COX measuring buffer and 20 mM ascorbate as electron donor. Increasing amounts of purified Cyt_c mutants (0-25 µM) were added, and oxygen consumption was recorded and analyzed with the Oxygraph software (Hansatech). The activity of COX was expressed as turnover number (TN) (s⁻¹) (Mahapatra et al., 2017).

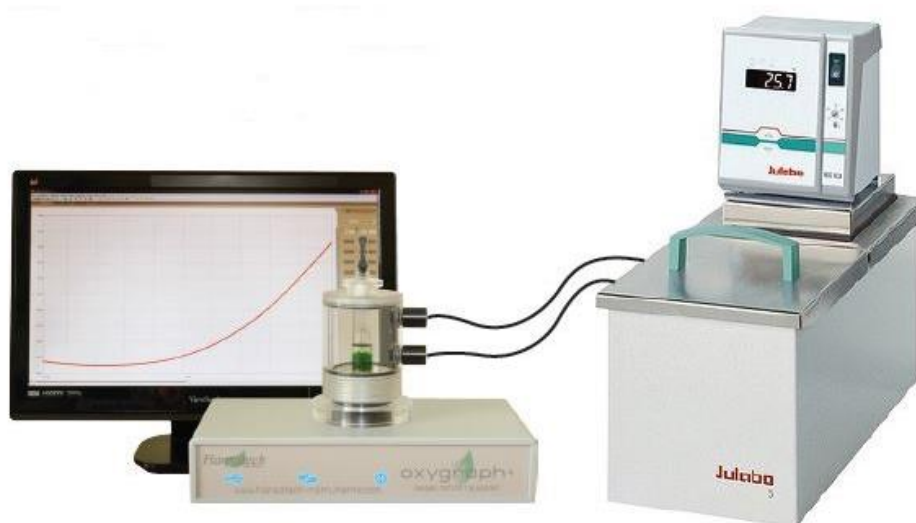


Figure 12. Hansatech Oxygraph Plus System connected to a water bath. Liquid-phase respiration measurement system. PC displays results real-time (0 to 4.5v analog output of oxygen electrode signal).

2.2.10. Measurement of Cytochrome *c* Redox Potential

The midpoint redox potential (E_0') was analyzed spectrophotometrically by the equilibration method described (Cammack, 1995) using 2,6-dichloroindophenol (DCIP, $E_0'=237$

mV) as a reference compound, which has an absorption band at 600 nm in its oxidized state. One hundred μL of Cyt c solution (2 mg/mL) was mixed in a spectrophotometric cuvette with 200 μL of 50 mM citrate buffer, pH 6.5, 10 μL of 1 mM DCIP, and 2.5 μL of 1 mM $\text{K}_3\text{Fe}(\text{CN})_6$ to fully oxidize Cyt c . Absorbance values corresponding to fully oxidized Cyt c (A_{550} - A_{570}) and DCIP (A_{600}) were recorded using a Jasco V-570 double beam spectrophotometer. The mixture was then sequentially reduced by adding 0.5 μL of 1 mM ascorbate (pH 6.5), and absorbance values were acquired at each step. When readings became constant, a few grains of sodium dithionite ($\text{Na}_2\text{S}_2\text{O}_4$) were added to fully reduce Cyt c and DCIP. For each step, ratios of oxidized and reduced forms of both compounds were calculated. Data obtained were plotted as $\log(\text{DCIP}_{\text{OX}}/\text{DCIP}_{\text{RED}})$ versus $\log(\text{Cyt}_{\text{OX}}/\text{Cyt}_{\text{RED}})$, yielding a linear graph with a slope of $n\text{-DCIP}/n\text{-Cyt}c$ and a y-axis intercept of $n\text{-Cyt}c / 59.2$ ($E_{\text{Cyt}c} - E_{\text{DCIP}}$). These values were used to calculate the E_0' (mV) of Cyt c from the Nernst equation (Pecina et al., 2010).

2.2.11. Measurement of Rates of Oxidation and Reduction

The kinetics of oxidation of 15 μM ferro-Cyt c variants with 50 μM H_2O_2 and reduction of 15 μM ferri-Cyt c variants with 200 μM ascorbate were measured spectrophotometrically at 550 nm as described (Liu et al., 2006). Cyt c mutants were reduced with sodium dithionite, and the proteins were separated from the reductant through NAP-5 columns (Catalog # 17-0853-02, GE Healthcare, Piscataway, NJ). Fifteen μM Cyt c in 0.2 M Tris-Cl, pH 7.0 were incubated with 50 μM oxidizing agent H_2O_2 and after 10 sec, the decrease of the absorption peak at 550 nm was measured, and the amount of oxidized Cyt c was calculated as described above. To measure the kinetics of reduction of Cyt c with ascorbate, Cyt c variants were fully oxidized with $\text{K}_3\text{Fe}(\text{CN})_6$ and purified using NAP-5 columns. Fifteen μM ferri-Cyt c were added to 50 mM sodium

phosphate, 25 mM sodium dithionite (Na_2SO_4), pH 7.0 and 200 μM ascorbate to a cuvette, which was then sealed from air, and the initial rate of reduction was measured at 550 nm (Mahapatra et al., 2017).

2.2.12. Measurement of Peroxidase Activity of Cytochrome *c* Mutants

Peroxidase activity of WT Cyt*c* variants were analyzed by their efficiency in the oxidation of a prototypical phenolic substrate, Amplex Red, to its product, resorufin as previously described by (Pecina et al., 2010). Cyt*c* variants with the concentration of 1 μM were incubated with liposomes containing TOCL/1,2-dioleoyl-sn-glycero-3-phosphocholine in a 1:1 ratio for 10 min. By the addition of Amplex Red (50 μM) and H_2O_2 (50 μM) the peroxidase reaction was started and was carried out for 20 min, while the rate of the reaction become linear. Fluorescence was detected by employing a “Fusion R” universal microplate analyzer by using an excitation wavelength of 535 nm and an emission wavelength of 585 nm (Mahapatra et al., 2017).

2.2.13. Crystallization of Cytochrome *c* Variants

Before crystallization, Cyt*c* was purified with DE52 and CM52 columns (Whatman, Piscataway, NJ). The proteins were concentrated by using Amicon Ultra-15 3k units (Catalog # UFC901008, Millipore, Billerica, MA), and buffer exchange with deionized water. The proteins were oxidized with 5 mM potassium ferricyanide to establish a defined oxidation state just before the crystallization. Crystallization was done by using Jena Biosciences basic screens. Protein concentration was approximately 15-20 mg/ml. Crystals were grown by vapor diffusion after mixing 1 μL of protein solution with 1 μL of the reservoir solution and equilibrating the drop against 0.5 mL of the precipitant at room temperature. Crystals were soaked for 10 min in a cryo-

protectant solution (20% v/v ethylene glycol) before flash freezing in liquid nitrogen. Single crystal diffraction data were collected at the Life Sciences Collaborative Access Team facility (Advanced Photon Source sector 21, Argonne National Laboratory). The data were collected over a full 360° rotation in either 0.6 or 1.0° frames and integrated using XDS (Kabsch, 2010) in Auto-Proc (Vonrhein et al., 2011).

2.2.14. Cell Culture

Mouse lung fibroblasts in which both the somatic and testes-specific *Cytc* isoforms have been knocked out, were cultured in high glucose Gibco Dulbecco's Modified Eagle Medium (Catalog # 11965-092, Thermo Fisher Scientific, Waltham, MA) supplemented with 1 mM sodium pyruvate, 50 µg/mL uridine, 10% fetal bovine serum with 1% penicillin-streptomycin at 37°C and 5% CO₂ (Mahapatra et al., 2017). Double knockout of *Cytc* is required because cultured mouse cells lacking somatic *Cytc* induce the expression of the testes isoform, restoring mitochondrial respiration (Vempati et al., 2007).

2.2.15. Transient Transfection and Selection of Double Knockout Mouse Lung Fibroblasts

The pBABE expression plasmid (Catalog # 1764, Addgene, Cambridge, MA) was used for the expression of *Cytc* variants in mammalian cells. The double knockout mouse lung fibroblasts were transfected with the empty vector (EV) control, the WT *Cytc*, and mutant constructs using TransFast transfection reagent (Catalog # E2431, Promega, Madison, WI) following the manufacturer's protocol. Cells were plated onto 100 mm culture dishes at a concentration of 1.3 x 10⁶ cells per dish a day before transfection. On the day of transfection, the TransFast reagent was mixed with the 10 µg of DNA at a ratio of 1:1 in serum- and antibiotic-free medium. Following

incubation at room temperature for 15 min, the mixture was overlaid onto the cells. The plates were incubated for 2 h at 37°C, and the cells were transferred to complete medium for 72 h and incubated at 37°C. Stable cell lines expressing WT, three *Cytc* variants, and an empty vector control were selected in the presence of 1.5 µg/mL puromycin.

CHAPTER 3

RESULTS

3.1 Cytochrome *c* is Acetylated on Lys53 in Prostate Cancer Xenografts

Mass spectrometry unambiguously revealed that Cyt c is acetylated on Lys-53 in both castrate-resistant (PC3) and castrate-sensitive (VCaP) tumors (Figure 13). Human Cyt c has 18 lysine residues; however, only Lys-53 residue contained an acetyl group in all 8-independent castrate-resistant and -sensitive prostate cancer xenografts (4 each). It is suggested that this is a cancer-specific modification. Importantly, phosphorylations, which are present in healthy tissues, were not detected in any of the tumor xenografts, indicating a dichotomy between signaling in normal and transformed cells that target Cyt c .

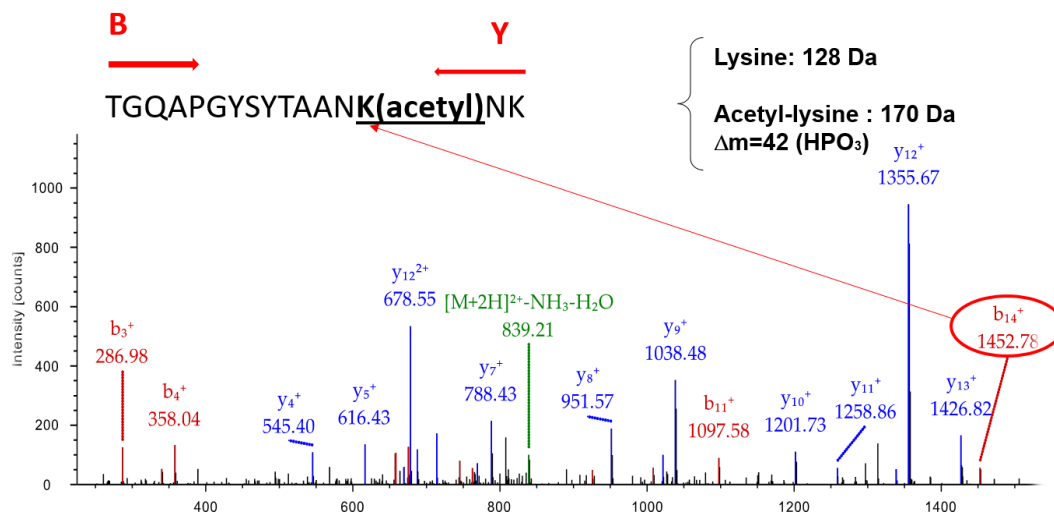


Figure 13. Nano-LC/ESI/MS/MS spectrum of TGQAPGYSYTAANKNK. Mass spectrum of Cyt c peptide TGQAPGYSYTAANK(acetyl)NK identifying Cyt c Lys-53 acetylation (underlined). For instance, one spectrum is shown from one castrate sensitive tumor xenograft. The acetyl moiety was unambiguously assigned to this lysine via fragment ions y_4^+ , y_5^+ etc. and b_{14}^+

containing 42 extra mass units for the acetyl group. The peptide sequence was unambiguously revealed by fragment ions b_3^+ , b_4^+ , b_{11}^+ , y_4^+ , y_5^+ , y_7^+ , y_8^+ , y_9^+ , y_{10}^+ , y_{11}^+ , y_{12}^+ , y_{12}^{2+} , and y_{13}^+ .

Additionally, Lys-53 is conserved in mammals (Zaidi et al., 2014) which points to a central regulatory site. The epitope surrounding Lys-53 was aligned with the Clustal Omega program (Figure 14) to visualize the conserved residue. Figure 15 shows the ribbon model of Cytc with Lys-53 residue highlighted.

	K53
Human	32 LHGLFGRKTGQAPGYSYTAAN <u>K</u> KNKGIIWGEDTLMEYLENPKKYI75
Bat	32 LHGLFGRKTGQAPGFSYTDAN <u>K</u> KNKGITWGEATLMEYLENSKKYI75
Dolphin	32 LHGLFGRKTGQAVGFSYTDAN <u>K</u> KNKGITWGEETLMEYLENPKKYI75
Mouse	32 LHGLFGRKTGQAAGFSYTDAN <u>K</u> KNKGITWGEDTLMEYLENPKKYI75
Rat	32 LHGLFGRKTGQAAGFSYTDAN <u>K</u> KNKGITWGEDTLMEYLENPKKYI75
Dog	32 LHGLFGRKTGQAPGFSYTDAN <u>K</u> KNKGITWGEETLMEYLENPKKYI75
Horse	32 LHGLFGRKTGQAPGFSYTDAN <u>K</u> KNKGITWKEETLMEYLENPKKYI75
Cow	32 LHGLFGRKTGQAPGFSYTDAN <u>K</u> KNKGITWGEETLMEYLENPKKYI75
Pig	32 LHGLFGRKTGQAPGFSYTDAN <u>K</u> KNKGITWGEETLMEYLENPKKYI75
Goat	32 LHGLFGRKTGQAPGFSYTDAN <u>K</u> KNKGITWGEETLMEYLENPKKYI75
	***** *.:*** ***** * * ***** ****

Figure 14. Cytc sequence alignment reveals that Lys-53 is conserved in mammals. The Clustal Omega program was used to align Cytc sequences. Lys-53 (bolded red and underlined) is conserved in all mammalian analyzed species. Identical amino acids are indicated with an asterisk.

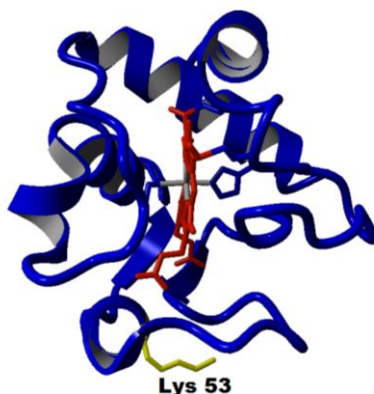


Figure 15. Ribbon model of cytochrome c. The heme group is shown in dark red. The Lys-53 residue is shown in yellow.

3.2 Sequence Confirmation of Cytochrome *c* mutants

To purify sufficient amounts of acetylated Cyt*c* *in vivo* for functional studies we would need about 500 g of prostate cancer tissue. Since the above method via tumor xenografts is cost-prohibitive, we applied a genetic approach instead. The effective and commonly used method to study the effects of protein acetylation *in vitro* is acetyl-mimetic substitution of an amino acid, i.e., replacement of the lysine with a glutamine residue. The acetyl-mimetic mutant mimics constitutive acetylation, converts the positive charge of the lysine to a neutral charge, similar to the effect of acetylation of a lysine residue that often results in functional changes like that seen with the acetylated protein *in vivo*. The bacterial pLWO1 and mammalian pBABE plasmids were used to generate WT Cyt*c*, acetyl-mimetic Lys53Gln, Lys53Arg (carries a positive charge, similar to non-acetylated lysine), and Lys53Ile (nonpolar/hydrophobic) as an additional control. The desired pLWO1 (Figure 16) and pBABE (Figure 17) Cyt*c* constructs were confirmed by sequencing. In the pLWO1 constructs there is only one single desired mutation of the Lys-53 residue. In the pBABE constructs there are two additional silent mutations which do not result in a change to the amino acid sequence of the protein.

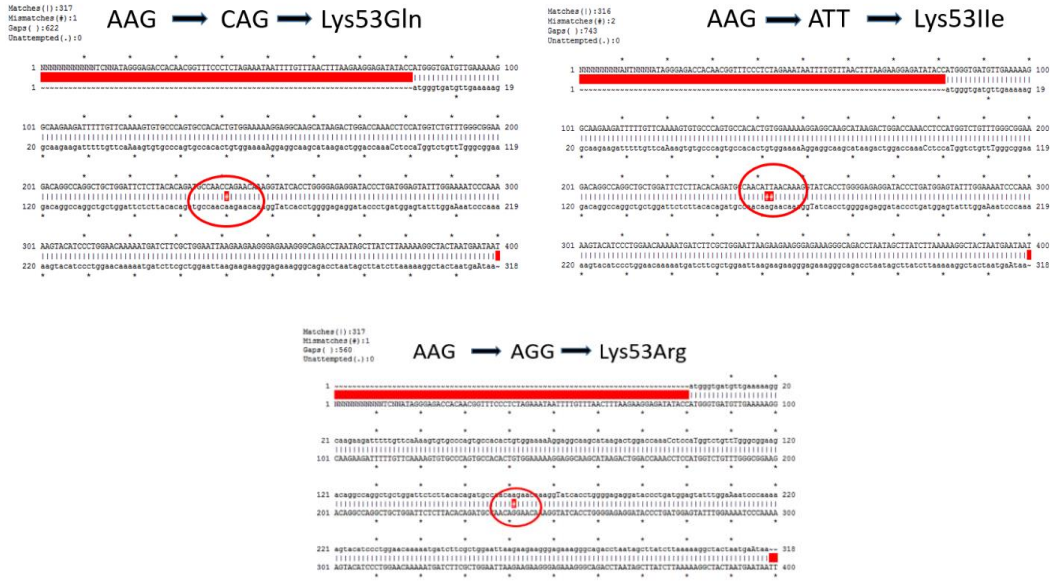


Figure 16. Sequence confirmation of pLWO1 cytochrome *c* constructs. The circled codons indicate the introduction of desired mutations on pLWO1 WT Cyt*c*. Cyt*c* Lys-53 was mutated to the Lys53Gln (acetylmimetic glutamine), Lys53Arg (cannot be acetylated), and Lys53Ile (nonpolar, as an additional control).

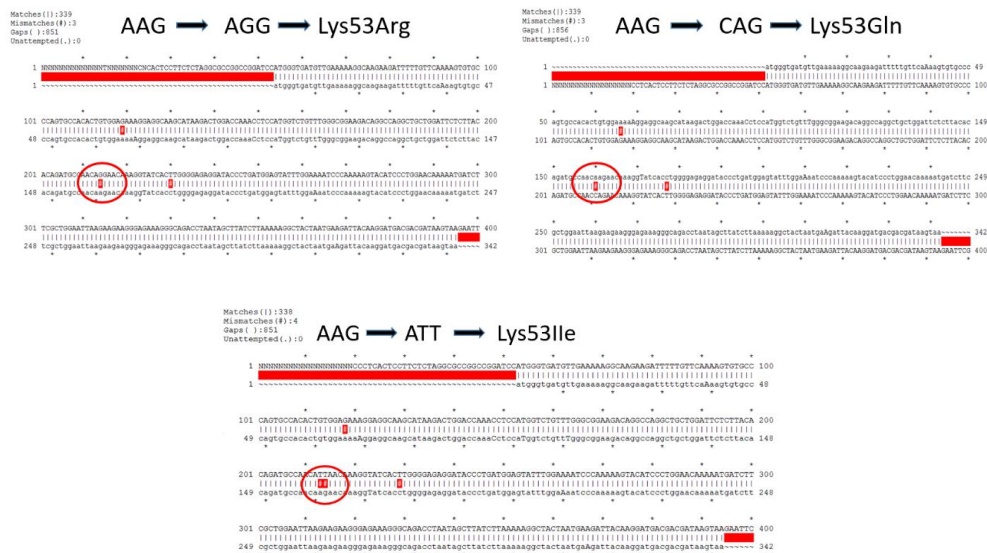


Figure 17. Sequence confirmation of pBABE cytochrome *c* constructs. The circled codons indicate the introduction of desired mutations on pBABE WT Cyt*c*. Cyt*c* Lys-53 was mutated to

the Lys53Gln (acetylmimetic glutamine), Lys53Arg (cannot be acetylated), and Lys53Ile (nonpolar, as an additional control).

3.3 Transient Transfection of Double Knockout Mouse Lung Fibroblasts

Double knockout mouse lung fibroblasts in which both the somatic and testes-specific *Cytc* isoforms have been knocked out, were confirmed by Western blot (Figure 18, KOLF). The absence of the band at 12 kD, and the presence of GAPDH loading control at 35 kD indicates that the cells are knocked out. The pBABE expression plasmid was used for the expression of *Cytc* variants in mammalian cells. The WT *Cytc* and mutant constructs were transfected into *Cytc* double knockout mouse lung fibroblasts. Cell lines expressing the three *Cytc* variants and an empty vector control were selected in the presence of 1.5 $\mu\text{g}/\text{mL}$ puromycin.

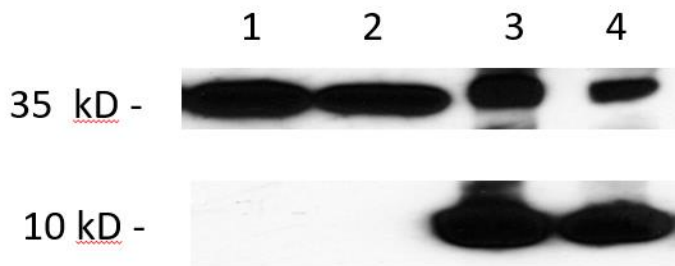


Figure 18. Western blot analysis of the double knockout mouse lung fibroblasts. Line 1-2, *Cytc*^{-/-} mouse lung fibroblasts (KOLF) cell lysates 100 and 75 ng/ μl ; Line 3-4, cow heart *Cytc* 100 and 75 ng/ μl respectively (Sigma, Western positive control).

3.4 Cytochrome *c* Variants were Overexpressed in *E. coli*

pLWO1 constructs confirmed by sequencing were used to transform competent *E. coli* C41 cells for protein overexpression and further purification by ion exchange chromatography. IPTG was used to induce the expression of *Cytc*. To check the protein expression level, 1 mL of culture

sample was harvested every 2 h. After 6 h induction, the small bacterial pellets showed a rich pink color (Figure 19), suggesting the presence of Cyt c protein.

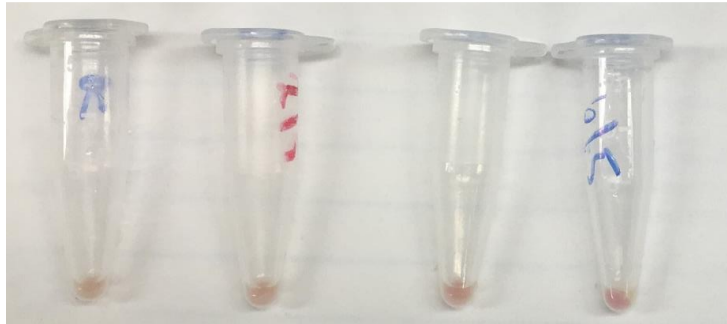


Figure 19. Overexpression of Lys53Gln cytochrome c after 0, 2, 4, and 6 hours IPTG induction. With the increase of IPTG induction hours, bacterial pellets acquire pink color, indicating the overexpression of Cyt c in *E. coli*.

Samples with 2, 4, and 6 h of induction were analyzed by Western Blotting with Sigma Cyt c as positive control, and Cyt c -/- cell lysates as a negative control (Figure 20). Bands at 12 kDa indicate the overexpressed Cyt c , and bands at 35 kDa indicate the GAPDH loading control for Cyt c -/- cell lysates. IPTG induction was stopped after 6 h. The large culture was centrifuged and the pink pellet (Figure 21) was stored at -80°C for further experiments.

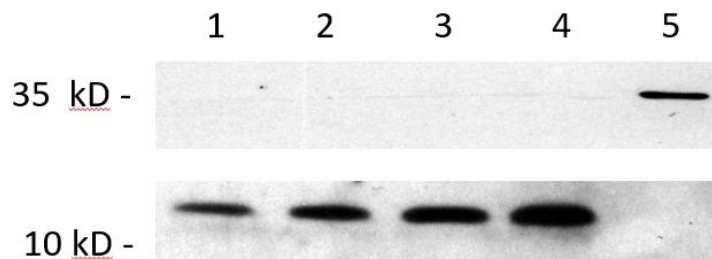


Figure 20. Western blot analysis of the overexpressed Lys53Gln cytochrome c after 2, 4, and 6 hours of IPTG induction. Lane 1, cow heart Cyt c (Sigma); lane 2, Lys53Gln Cyt c after 2h

IPTG induction; lane 3, Lys53Gln Cyt c after 4h IPTG induction; lane 4, Lys53Gln Cyt c after 6h IPTG induction; lane 5, Cyt c -/- cell lysates (Western negative control).



Figure 21. Bacterial pellets of the overexpressed Lys53Gln cytochrome c . Bacterial pellets from a large culture showed a rich pink color after 6 hours of IPTG induction.

3.5 Concentration Determination and Purification of Functional and Correctly Folded Cytochrome c Variants from *Escherichia coli*

Overexpressed WT, Lys53Gln, Lys53Arg, and Lys53Ile Cyt c were purified in a two-step ion-exchange chromatography with DE52 anion-exchange and CM52 cellulose cation-exchange columns. After protein concentration, the yields of proteins vary from 15 - 25 mg/mL. The purity of proteins was analyzed spectrophotometrically, with 410 nm/280 nm ratios > 4 as an indicator and marker value of Cyt c purity (Patel et al., 2001). The WT Cyt c and all three mutants were fully reducible according to the absorption spectra measurements (Figure 22). Additionally, the presence of the weak 695 nm absorption peak in the oxidized state of Cyt c variants suggest that all mutant and WT proteins were purified in the correctly folded conformation (state III) (Figure 22, insert). This peak is caused by the interaction between Met-80 and the heme iron. It called as

an “indicator of trouble” since it is usually lost after any harmful treatment, which leads to denaturation of Cyt c (Dickerson and Timkovich, 1975).

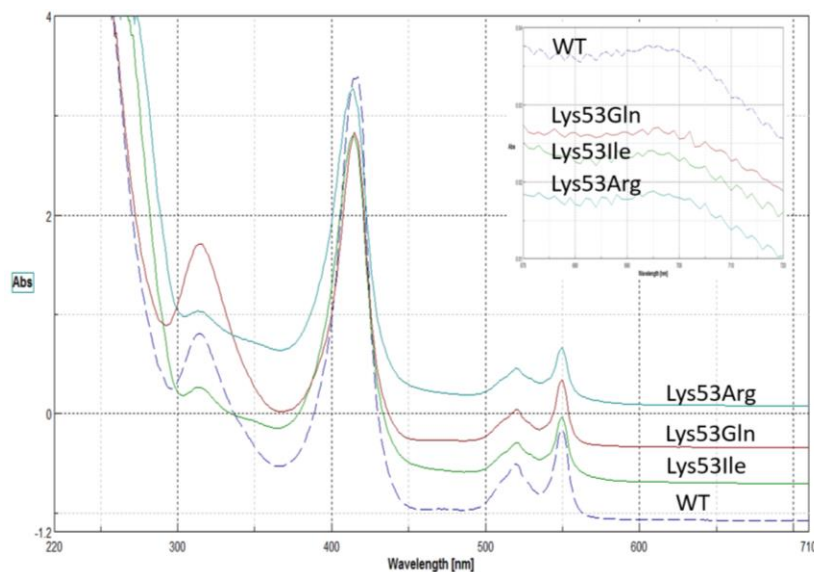


Figure 22. Purified cytochrome c mutant's absorption spectra. One hundred μM of WT, Lys53Arg, Lys53Gln, and Lys53Ile overexpressed proteins were oxidized with $\text{K}_3\text{Fe}(\text{CN})_6$ and desalted via NAP-5 columns. Absorption spectra were recorded on a Jasco V-570 double beam spectrophotometer (2 nm bandwidth, 200 nm/min scanning speed). Reduced Cyt c proteins were obtained by adding few granules of sodium dithionite. **Insert:** The weak 695 nm absorption band of oxidized Cyt c .

3.6 Acetylmimetic Lys53Gln Cytochrome c Mutant Exhibits a Decrease in Respiration Rate with Isolated Cytochrome c Oxidase

The hallmarks of cancer growth are increased glycolysis and lactate production. Malignancies and tumor cell expansion are also characterized by mitochondrial respiration deficits and depletion of OXPHOS. Therefore, we proposed that acetylation state of Cyt c triggers an inhibition of mitochondrial respiration and causes the metabolic switch, the Warburg effect. To

test the hypothesis that Cytc acetylation leads to inhibition of respiration, we analyzed the activity of purified COX with purified Cytc variants as substrates. COX was previously isolated from bovine liver under conditions that preserve phosphorylation status *in vivo* and yield a regulatory competent enzyme (Lee et al., 2009). Oxygen consumption of 0.15 μM bovine liver COX was measured using a Clark type oxygen electrode system at 25°C with titrations (1-25 μM) of purified Cytc variants. The experimental results demonstrated that COX oxidizes acetylmimetic Lys53Gln and nonpolar Lys53Ile Cytc mutants at lower rates compared to the WT Cytc and Lys53Arg control mutant (Figure 23). The kinetics of Cytc oxidation by COX revealed that maximal velocity of acetylated Cytc reduced by approximately 50% compared to the WT. The data suggest that acetylation of Cytc down-regulates mitochondrial ETC electron flux and leads to inhibition of respiration. These results could also deepen the understanding of the molecular pathways leading to mitochondrial inhibition and metabolic switching during tumorigenesis, i.e., Warburg metabolism.

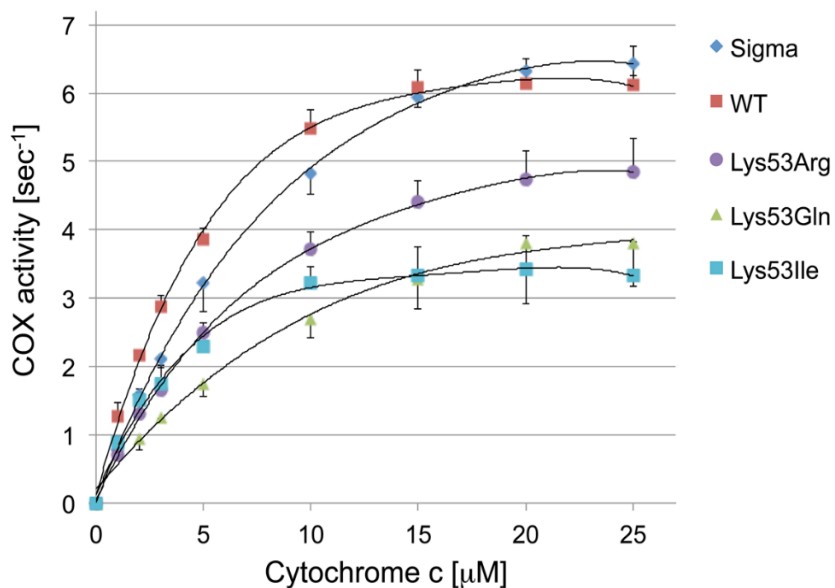


Figure 23. Measurements of Cytochrome *c* oxidase activity with purified cytochrome *c* mutants. V_{max} of acetylmimetic Lys53 mutant decreased by approximately 50% with the

comparison to the WT *Cytc*. Data is expressed as turnover number (sec^{-1}). Shown are representative measurements ($n=3$).

3.7 Acetylmimetic Lys53Gln Cytochrome *c* is Incapable to Activate Caspase-3 and Turns off Apoptosis

Apoptosis is a mechanism by which damaged cells are programmed to cell death and to commit suicide. Cancer cells manage to bypass this mechanism and are able to evade apoptosis. Considering the crucial role of *Cytc* in programmed cell death, we hypothesized that acetylation of *Cytc* could lead to inhibition of apoptosis in cancer cells. To test the hypothesis, we analyzed the ability of *Cytc* variants to initiate the programmed cell death by downstream activation of Caspase-3. 15 $\mu\text{g}/\text{mL}$ of purified WT *Cytc*, Lys53Gln, Lys53Arg, and Lys53Ile mutants were incubated with 2 mg/mL of cytosolic extract from HeLa cells for 2.5 hours at 37°C . The activity of caspase-3 was measured by following cleavage of the artificial substrate DEVD coupled to fluorescent rhodamine. Interestingly, the results indicated that acetylmimetic Lys53Gln and nonpolar Lys53Ile *Cytc* mutants were unable to trigger caspase-3 activity and induce apoptosis, compared to WT. Interestingly, the Lys53Arg *Cytc* control mutant demonstrated higher activity of caspase-3 activation and ability to execute apoptosis than WT *Cytc* (Figure 24). Our data suggests that acetylation of *Cytc* affects protein function at the apoptosome formation level, and modification of the key regulatory epitope of *Cytc* turns off the programmed cell death. This result could potentially establish the mechanisms underlying evasion of apoptosis in prostate cancer.

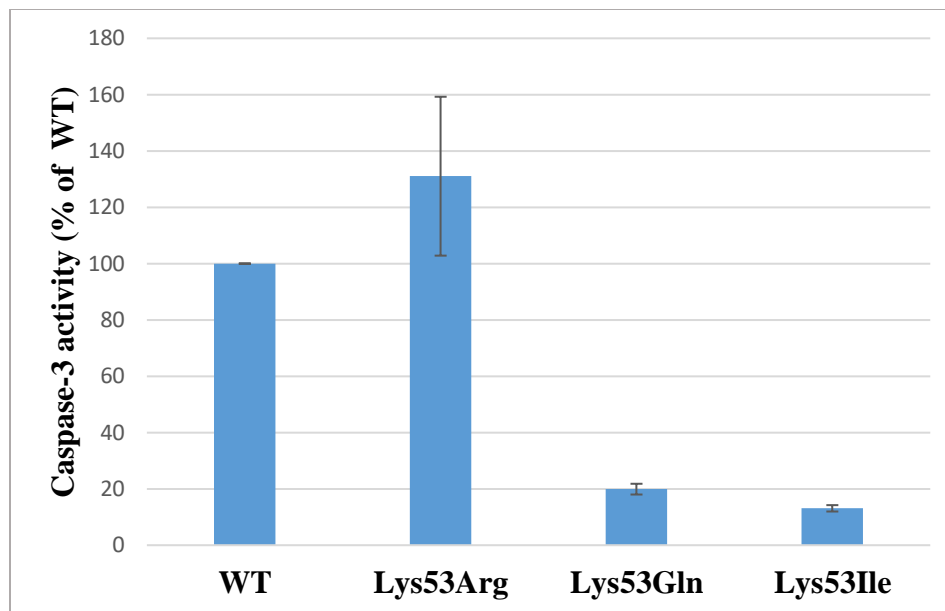


Figure 24. The ability to trigger downstream caspase-3 activation is strongly inhibited in cytochrome *c* acetylmimetic Lys53Gln and nonpolar control Lys53Ile mutants *in vitro*. Cleavage of the artificial caspase-3 substrate DEVD-R110 via induced caspase-3 was measured in 10 μ L aliquots of preincubated Cytc variants and HeLa cell cytosolic fractions (n=3).

3.8 Assessments of Peroxidase Activity of Cytochrome *c* Mutants

Cytc plays role in cardiolipin peroxidation. Cytc binds to cardiolipin and this interaction causes partial unfolding of the enzyme, as well as making the bond between the heme group and Met-80 weaker, unleashing its peroxidase activity. Peroxidation of cardiolipin and other lipids leads to damage of the mitochondrial membrane, which enhances the release of Cytc from the mitochondria during apoptosis.

Peroxidase activity of the Cytc variants was analyzed by their efficiency to oxidize cardiolipin (CL) reconstituted in vesicles, which after oxidation oxidizes a prototypical phenolic substrate, Amplex Red, to its product, resorufin. Thus, assessment of peroxidase activity with Amplex Red was performed by measuring the fluorescence of resorufin, an oxidation product of

Amplex Red. 1 μM of Cyt c was incubated with liposomes containing TOCL/DOPC at a ratio 1:1 for 10 min. The peroxidase reaction was started by the addition of 50 μM Amplex Red and 50 μM H_2O_2 and was carried out for 20 min (reaction rate was linear during the entire time interval). Fluorescence was detected by employing a “Fusion R” universal microplate analyzer and by using an excitation wavelength of 535 nm and an emission wavelength of 590 nm. The data showed that the peroxidase activity of the acetylmimetic Lys53Gln and nonpolar Lys53Ile Cyt c mutants were slightly lower than that of the WT Cyt c . Interestingly, the peroxidase activity of Lys53Arg Cyt c mutant was higher than the activity of the WT, suggesting that it unfolds more easily than WT and the Lys53Gln and Lys53Ile mutants (Figure 25). These findings align with the apoptotic assay results. The Lys53Arg Cyt c mutant demonstrated the highest ability to activate caspase-3 and induce apoptosis, while acetylmimetic Lys53Gln and nonpolar Lys53Ile were incapable of triggering apoptosis.

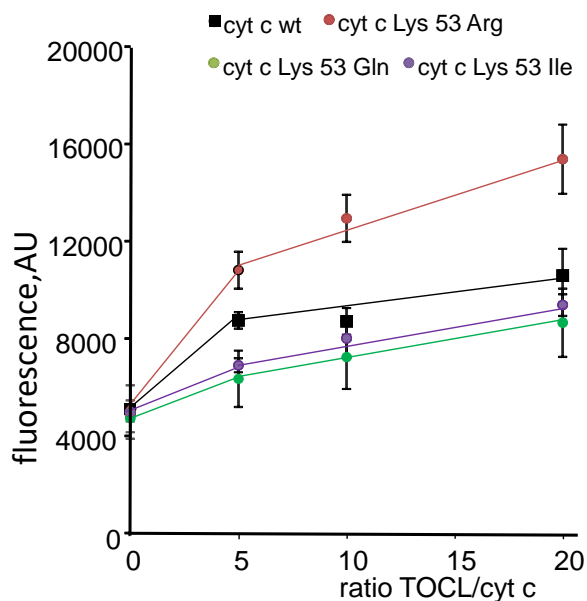


Figure 25. Peroxidase activity of the cytochrome c variants. Assessment of peroxidase activity with Amplex Red reagent was performed by measuring the fluorescence of resorufin, an oxidation product of Amplex Red.

3.9 Measurement of Redox Potential of Cytochrome *c* Mutants

Cytc is an electron carrier between complex III and complex IV in the ETC. For the proper protein function, Cytc redox potential should be in the range between the redox potential of complexes III and IV. The literature values of mammalian Cytc redox potential are in the range of 220-270 mV (Cammack, 1995; Nicholls and Ferguson, 1992). The enzyme midpoint redox potential (E^0) of purified Cytc variants was measured spectrophotometrically via the equilibration method using DCIP as substrate. The average redox potential of WT Cytc was 256 mV which is similar to the literature value. Cytc mutant's values were 254 for Lys53Gln, 250 for Lys53Arg, and 261 for Lys53Ile, which are in range between the redox potential of complex III and IV (Figure 26). The results suggest the thermodynamic feasibility of Cytc mutant's proper function within the respiratory chain.

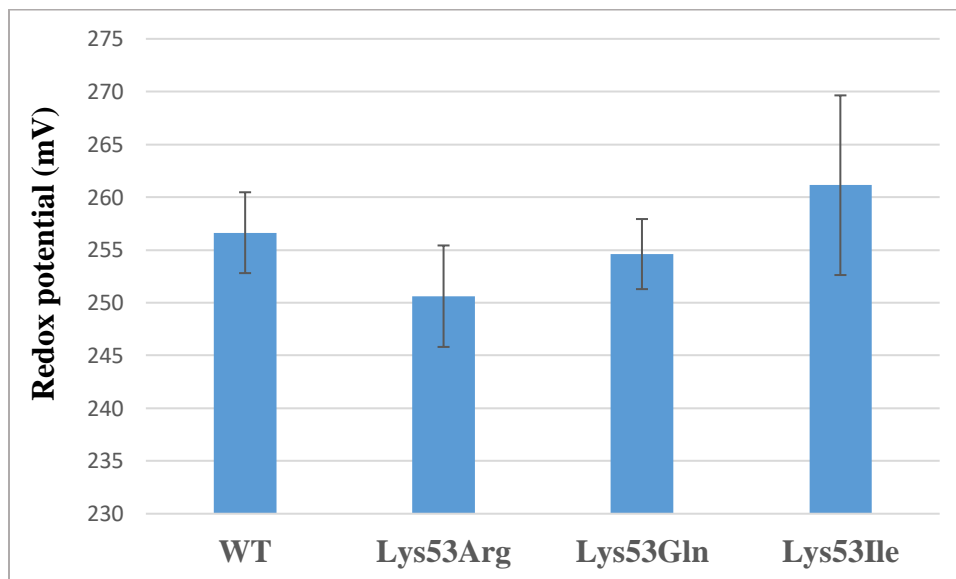


Figure 26. Measurement of cytochrome *c* mutant's redox potential. Data were plotted as $\log(\text{DCIP}_{\text{ox}}/\text{DCIP}_{\text{red}})$ versus $\log(\text{Cyt}_{\text{ox}}/\text{Cyt}_{\text{red}})$ yielding a linear graph and Redox potentials were calculated using the Nernst equation from the intercept and slope of the graph. Final redox potential values are shown (n=5).

3.10 Measurement of Rates of Oxidation and Reduction of Cytochrome *c* Mutants

As described above, Cyt c is able to function as a radical scavenger within the mitochondrial inner-membrane space. The reduction of Cyt c by superoxide, or oxidation of Cyt c by H₂O₂ can regenerate the molecule of oxygen by removing electrons. Considering the antioxidant role of Cyt c , we tested the ability of Cyt c variants in the reaction with H₂O₂ and with the reductant ascorbate.

To determine the rate of Cyt c oxidation, Cyt c variants were reduced with sodium dithionite, followed by removal of reductant via NAP-5 columns. The ferro-(Fe²⁺)-Cyt c variants were oxidized in the presence of 50 μ M H₂O₂. The Lys53Gln acetylmimetic mutant was oxidized at about twice the rate compared to WT and Lys53Arg Cyt c controls, while the Lys53Ile mutant showed a 2.83-fold higher rate (Figure 27).

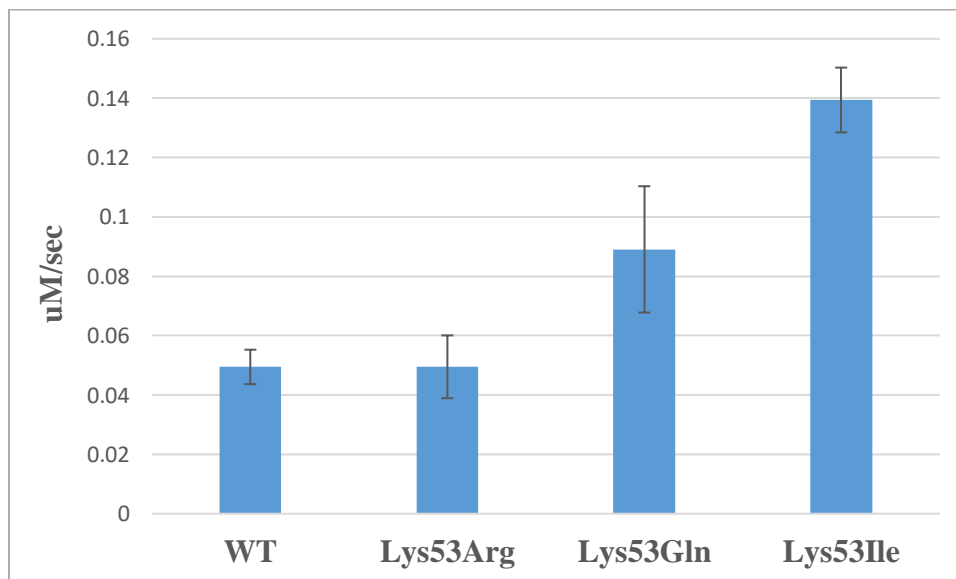


Figure 27. Cytochrome *c* variants' oxidation rate. The oxidation rate of the Lys53Gln and Lys53Ile Cyt c mutants were increased approximately two - and threefold, respectively, compared to WT and Lys53Arg Cyt c in the presence of H₂O₂ (n=7).

The reduction rate of Cyt c variants was determined with the reductant ascorbate. Cyt c variants were oxidized with $K_3Fe(CN)_6$ and desalted with NAP-5 columns. Ferri-(Fe^{3+})-Cyt c mutants were then reduced with 200 μ M ascorbate. The acetylmimetic Lys53Gln and nonpolar Lys53Ile mutants were reduced at a much faster rate compared to WT and Lys53Arg Cyt c controls (Figure 28). Taken together, our data suggest that the acetylmimetic Cyt c can act as a good single electron donor and acceptor, thus, effectively scavenging ROS, which could be a selective advantage with acetylated Cyt c for cancer cells which often face a high ROS load.

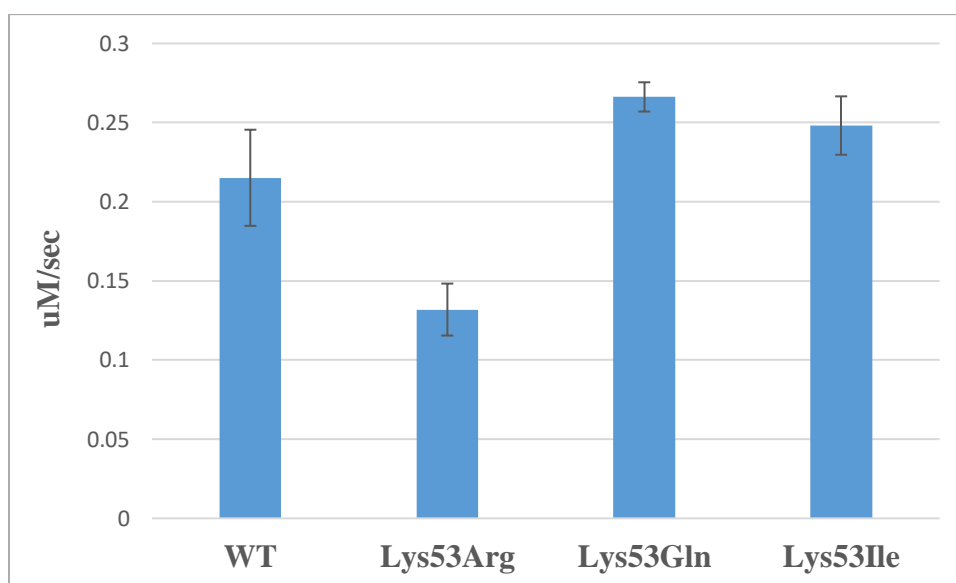


Figure 28. Cytochrome c variants' reduction rate. The reduction rate of Lys53Gln and Lys53Ile Cyt c mutants were increased compared to WT and Lys53Arg Cyt c in the presence of ascorbate (n=7).

3.11 Crystallization of Cytochrome c Variants

The best diffracting crystals of Lys53Gln mutant (Figure 29) grew to 0.3x.1mm size in plates in JBS1D4 condition which was 30% PEG 2K MME, 0.1M MES 6.5 and 0.1M Na-acetate. Figure 30 shows the components in the crystal structure of the Lys53Gln mutant that are within

3.5 Å of Gln53 in molecules A and B. The electron density from an unbiased “omit” map is shown at 1.0 sigma. The electron density for Gln-53 in molecule B is better defined because its side chain is immobilized by a hydrogen bond to the carbonyl oxygen of Tyr-40. The side chain of Gln-53 in molecule A interacts only with a water molecule within 3.5 Å.

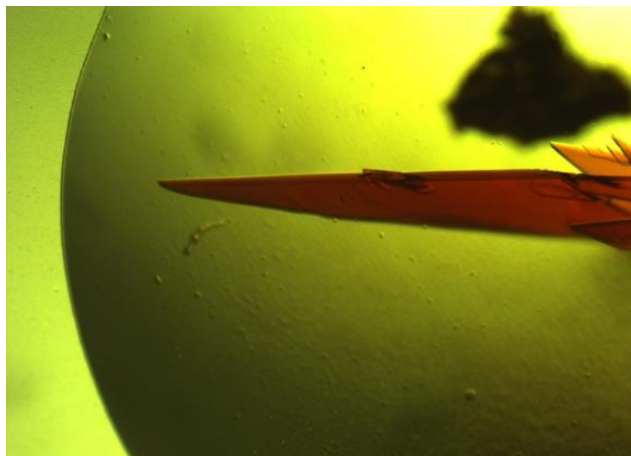


Figure 29. Crystal of the Lys53Gln cytochrome *c* mutant.

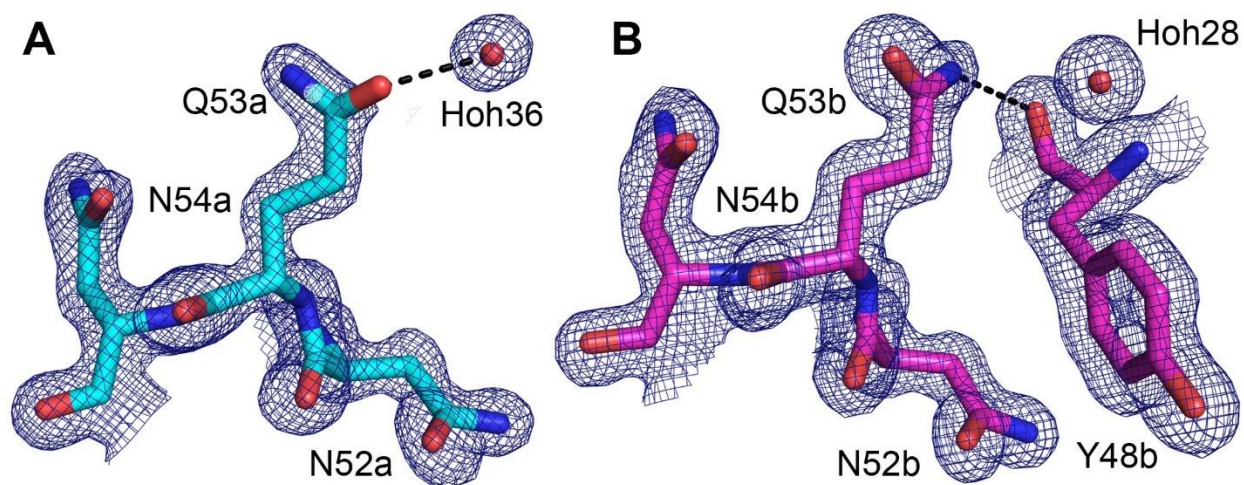


Figure 30. The comparison of the “omit” density for the Lys53Gln in the two cytochrome *c* molecules in the asymmetric unit of the crystal structure.

The crystal structure of the Lys53Gln Cyt c (blue) was superposed onto the structure of the native (5C0Z.pdb) cytochrome c (green) using only the A-chains in both structures (Figure 31). The four independent chains in the native structure are labeled with lower case letters. The two independent chains in the Lys53Gln Cyt c structure are labeled with capital letters. The RMSD value for the superposed A-chains was 0.35 Å calculated from the backbone atoms. The protein structures are depicted as C α traces with the atoms in the hemes and the ferrihexacyanide molecules represented by spheres. Panel A shows the front face of the 5C0Z tetramer in the P1 asymmetric unit. Panel B shows the edge of the tetramer after a 90° rotation about the vertical axis. When the two structures are superposed using only the A-chains, the B-chain in the Lys53Gln Cyt c structure partially overlaps with the D-chain in 5C0Z but their relative orientation in the two crystal structures differs dramatically (RMSD = 20.3 Å). The crystallographic parameters for the Lys53Gln structure are compared to those of the native mouse Cyt c (5C0Z.pdb) and the Y47F human Cyt c (3ZOO.pdb) structures in Table 3 below.

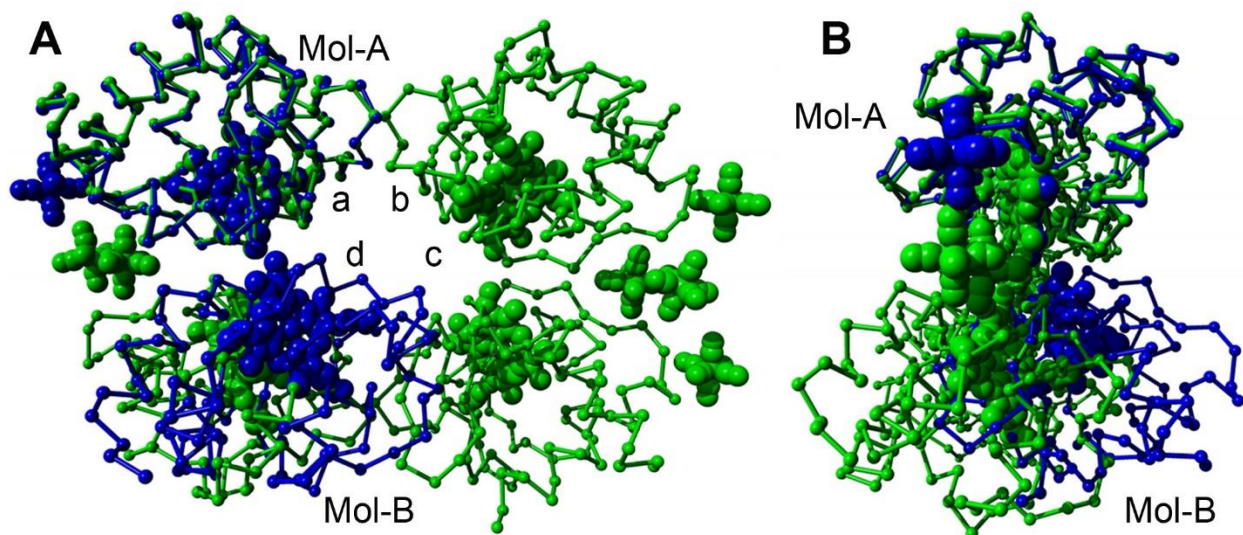


Figure 31. The structure of Lys53Gln cytochrome c is superposed onto the native mouse/rat cytochrome c (5C0Z.pdb) using chain-A in both structures. The structure of Lys53Gln cytochrome c shown in blue, and native mouse/rat cytochrome c (5C0Z.pdb) shown in green.

Table 3. Crystallographic data summarizing and comparing three structures of mouse / rat cytochrome *c*: Native, K53Q, and human Y46F.

STRUCTURE	CYTC MOUSE	CYTC (K53Q) MOUSE	CYTC (Y47F) HUMAN
PDB CODE	5C0Z	N/A	3ZOO
DATA CODE	141118x21a	161109x06a	
CRYSTALLIZATION			
Iron	Oxidized	Oxidized	Oxidized
Protein	15 mg/mL Cyt c (WT) + 5mM K ₃ Fe(CN) ₆ in water	17mg/mL Cyt c (K53Q) + 5mM K ₃ Fe(CN) ₆ in water	12.5 mg/ml oxidized Cyt c in 22.5% (w/v) PEG-1000, 50 mM KH ₂ PO ₄ , pH 7.0
Well	25% PEG 4K, 8% iso propanol, 0.1M Na Acetate, pH 6.5	30% PEG 2K MME, 0.1M Na MES, 0.1M Na Acetate, pH 6.5	26-31% (W/V) PEG 1000, 40 mM, KH ₂ PO ₄ . pH 7.0
Drop	1:1 Protein:Well	1:1 Protein:Well	n/a
Cryoprotectant	30% PEG 4K, 8% isopropanol, 0.1M Na Acetate, 20% Ethylene glycol, 10 min soak with 5mM	35% PEG 2K MME, 0.1M Na MES, 0.1M Na Acetate, pH 6.5, 20% Ethylene glycol	26-31% (w/v) PEG 1000, 40 mM, KH ₂ PO ₄ , 15% Glycerol, pH 7.0

	K ₃ Fe(CN) ₆ , final ph 6.5		
CRYSTAL DATA			
Space group:	P1	P2(1)2(1)2	P1
Unit cell: a	34.401	53.055	36.367
b	52.471	96.911	53.952
c	61.647	38.072	58.95
Alpha	110.04	90	76.55
Beta	92.77	90	88.73
Gamma	92.02	90	71.86
Chains per A.U.	4	2	4
Matthews Coeff	2.24	2.10	2.3
Solvent %	45.12	41.4	46.7
X-RAY DATA			
Resolution-high (Å)	1.12	1.31	1.35
Resolution-low (Å)	49.22	48.38	30.59
Beamline	APS 21-ID-F	APS 21-ID-D	DIAMOND 103 (UK)
Wavelength	0.97872	1.07822	0.9762
Reflections	127840	48257	81707
Completeness	87.4 (44.7)	98.9 (86.8)	94.7 (80.7)
Average I/sigma	14.4 (2.0)	12.2 (2.1)	8.70 (n/a)
Redundancy	3.9 (3.7)	11.1 (6.6)	n/a

Rmerge	0.050 (0.548)	0.120 (0.821)	0.07
REFINEMENT			
Rfactor	0.132 (0.239)	0.146 (0.352)	0.138
Rfree	0.159 (0.240)	0.181 (0.364)	0.179
Avg B-factor (Å²)	15.97	21.19	17.703
Protein atoms per A.U.	3228	1917	3981
Water molecules	537	388	417
Bond RMSD	0.017	0.021	0.017
Angle RMSD	1.903	2.372	1.99
FC6 OCCUPANCY			
202a/A	0.28	0.50	
202b/A	0.37		
202/B	0.93		
203/B	–	–	
203a/B	0.30		
203b/B	0.32		
202/C	0.90		
HEME LINKS: Average (Å)			
C14 SG - HEM CAB	1.90 (0.04)	1.74 (0.01)	1.95 (0.02)
C17 SG - HEM CAC	1.98 (0.04)	1.86 (0.00)	2.13 (0.07)
H18 NE2 - FE2 (Å)	2.02 (0.01)	1.99 (0.01)	2.02 (0.03)
M80 SD - FE2 (Å)	2.30 (0.01)	2.31 (0.01)	2.28 (0.02)

CHAPTER 4

SUMMARY

4.1 Discussion and Conclusion

This research is focused on the basic science underlying prostate cancer. Prostate cancer is a heterogeneous disease and one of the most typical cancer types in men. It is very difficult to diagnose carcinoma early, as there are no symptoms in the early stages. Therefore, prostate cancer is the second leading cause of cancer-related death in men in the US. Cancer progression classically follows the Warburg effect, a metabolic switch from depending primarily on mitochondrial respiration to depending primarily on glycolysis, even in oxygen-rich conditions. Another hallmark of cancer is that cancer cells manage to evade apoptosis. Even after more than 70 years of cancer research, a full understanding of the underlying mechanism has not yet been achieved.

Cell signaling, via post translational modifications (PTMs), is one of the most important means of regulation in higher organisms. Cell signaling is also most commonly dysregulated in different types of cancer, including prostate cancer, in which androgen signaling plays a crucial role in driving cell proliferation. Cancer cells use mitochondria as signaling organelles, for cancer bioenergetics, and biosynthesis of macromolecules.

In higher organisms, energy metabolism is completely dependent on mitochondrial OXPHOS, including the electron transport chain (ETC), which is also the main source of ROS. *Cytc*, a small heme protein, is an essential component of the ETC where it plays an important role in generation of cellular ATP and ROS. *Cytc* also plays another crucial role in type II apoptosis. When *Cytc* is released from the mitochondria into the cytosol, it binds to Apaf-1 and activates downstream caspases. Despite the central role of *Cytc* in respiration, apoptosis, and ROS formation

or scavenging, very little is known about the regulation of its functions. Recent studies indicated that Cyt c can be posttranslationally modified and regulated through cell signaling pathways. It was shown that phosphorylation of Cyt c under healthy conditions decisively regulates the protein functions, including respiration and apoptosis.

To date, no study has been performed to investigate structural and functional changes of Cyt c in cancer, a major gap in knowledge. In this study, we hypothesized that the development of prostate cancer causes changes in Cyt c posttranslational modifications, which in turn alter the main functions of Cyt c . Importantly, our preliminary data demonstrate that human Cyt c is acetylated on lysine 53 residue in human prostate tumor xenografts grown in mice. Mass spectrometry unambiguously assigned the acetylation site to Lys-53 in both castrate-resistant and -sensitive tumors. This is the first time that Cyt c acetylation has been identified in mammals. Strikingly, Lys-53 is the single and only lysine residue that contained an acetyl group in eight independent tumor xenografts, suggesting that this is a cancer-specific modification. Therefore, we hypothesized that in prostate cancer the acetylation state of Cyt c changes from a “healthy” to a “cancer” state, where inhibition of mitochondrial respiration leads to the Warburg effect. To characterize the effects of acetylation *in vitro*, Lys-53 was mutated to the acetylmimetic glutamine, a non-acetylated arginine that carries a positive charge, and to the nonpolar isoleucine as an additional control. Cyt c variants were overexpressed in bacteria and purified to homogeneity. The Lys53Gln mutant crystallized and gave a high resolution structure at 1.31 Å that showed good omit map density for Gln53 and confirmed that the mutation caused no significant modification of the overall structure. We were able to show with acetylmimetic Cyt c that this modification strongly inhibits the participation of Cyt c in apoptosis.

To test the hypothesis that acetylation of *Cytc* leads to inhibition of mitochondrial respiration, COX activity was analyzed with purified *Cytc* variants. Compared to WT, the acetylmimetic Lys53Gln and nonpolar Lys53Ile *Cytc* mutants showed a 50% decrease in respiration. These findings support the hypothesis that acetylation of *Cytc* down-regulates mitochondrial electron flux, decreases cell respiration, and leads to the Warburg effect in cancer. To check that the acetylation of *Cytc* leads to inhibition of apoptosis in cancer, we examined the ability of *Cytc* variants to activate Caspase-3. Remarkably, the acetylmimetic Lys53Gln and nonpolar Lys53Ile *Cytc* were incapable to trigger a robust caspase-3 activation and thus, to induce apoptosis. The suppression of apoptosis agrees with the observation that the Lys-53 epitope is directly involved in the interaction between *Cytc* and Apaf-1 (Cheng et al., 2016; Zhou et al., 2015).

Furthermore, we assessed the cardiolipin peroxidase activity of *Cytc* variants with Amplex Red by measuring the fluorescence of resorufin, an oxidation product of Amplex Red. The acetylmimetic Lys53Gln and nonpolar Lys53Ile *Cytc* mutants had lower peroxidase activity than that of WT *Cytc*. Interestingly, the peroxidase activity of the Lys53Arg mutant was higher than the activity of the WT, suggesting that it unfolds more easily than WT and the Lys53Gln and Lys53Ile *Cytc* mutants. This data correlates with the apoptotic results, where Lys53Arg *Cytc* mutant demonstrated the highest ability to activate caspase-3 and induce apoptosis, while acetylmimetic Lys53Gln and nonpolar Lys53Ile showed a very little ability to trigger apoptosis.

As expected, we observed that the redox potentials of the *Cytc* variants were in a range between the redox potential of complex III and IV, suggesting the thermodynamic requirement of the proteins to properly function within the ETC. The oxidation and reduction rates of *Cytc* mutants were measured in the reactions with H₂O₂ and the reductant ascorbate. The acetylmimetic Lys53Gln and nonpolar Lys53Ile *Cytc* mutants were oxidized at about twice the rate compared to

the WT and Lys53Arg *Cytc* controls, suggesting their higher ability to degrade H₂O₂ and act as a stronger ROS scavenger compared to WT. In the reaction with ascorbate, Lys53Gln and Lys53Ile *Cytc* were reduced at a much faster rate compared to WT and Lys53Arg *Cytc* controls. Their higher ability to accept electrons further supports their ROS scavenging capacity.

We conclude that cancer signaling leads to a change in the *Cytc* acetylation state, causing an inhibition of respiration ("Warburg effect"). It also renders *Cytc* incapacitated of triggering apoptosis, allowing cancer cells to evade programmed cell death.

4.2 Future Directions

A translational goal of this work is to improve future diagnosis and therapy, by using *Cytc* acetylation as a predictive biomarker and by targeting the to-be-identified acetylase/deacetylase, respectively. It is likely that the extent of *Cytc* Lys53 acetylation correlates with cancer aggressiveness. The first step to test this hypothesis would be a development of a monoclonal antibody and to test them on a panel of cancer specimens.

Another important project direction would be to functionally characterize acetylmimetic *Cytc* in the mammalian cell culture system. To further confirm the results, mitochondrial function would be analyzed in intact cells. Such future studies will include experiments to examine mitochondrial membrane potential and ROS production, aconitase activity as a marker of oxidative stress, and ROS scavenging markers including MnSOD, CuZnSOD and glutathione peroxidase. Additional metabolic readouts will be ATP and lactate production.

Efforts will continue to determine the crystal structures of the Lys53Ile and Lys53Arg *Cytc* mutants to see if they help explain the functional differences reported in this study. Molecular

dynamics calculations, similar to those analyzed in (Mahapatra et al., 2017) might also elucidate the differences.

REFERENCES

- Acin-Perez, R., Bayona-Bafaluy, M.P., Bueno, M., Machicado, C., Fernandez-Silva, P., Perez-Martos, A., Montoya, J., Lopez-Perez, M.J., Sancho, J., and Enriquez, J.A. (2003). An intragenic suppressor in the cytochrome c oxidase I gene of mouse mitochondrial DNA. *Hum Mol Genet* *12*, 329-339.
- Allen, S., Balabanidou, V., Sideris, D.P., Lisowsky, T., and Tokatlidis, K. (2005). Erv1 mediates the Mia40-dependent protein import pathway and provides a functional link to the respiratory chain by shuttling electrons to cytochrome c. *J Mol Biol* *353*, 937-944.
- Anderson, K.A., and Hirschey, M.D. (2012). Mitochondrial protein acetylation regulates metabolism. *Essays Biochem* *52*, 23-35.
- Auburger, G., Gispert, S., and Jendrach, M. (2014). Mitochondrial acetylation and genetic models of Parkinson's disease. *Prog Mol Biol Transl Sci* *127*, 155-182.
- Baeza, J., Smallegan, M.J., and Denu, J.M. (2016). Mechanisms and Dynamics of Protein Acetylation in Mitochondria. *Trends Biochem Sci* *41*, 231-244.
- Beckman, J.S., and Koppenol, W.H. (1996). Nitric oxide, superoxide, and peroxynitrite: the good, the bad, and ugly. *Am J Physiol* *271*, C1424-1437.
- Belikova, N.A., Vladimirov, Y.A., Osipov, A.N., Kapralov, A.A., Tyurin, V.A., Potapovich, M.V., Basova, L.V., Peterson, J., Kurnikov, I.V., and Kagan, V.E. (2006). Peroxidase activity and structural transitions of cytochrome c bound to cardiolipin-containing membranes. *Biochemistry* *45*, 4998-5009.
- Brems, D.N., and Stellwagen, E. (1981). The effect of methylation on cytochrome c fragment complementation. *J Biol Chem* *256*, 11688-11690.
- Cadenas, E., and Davies, K.J. (2000). Mitochondrial free radical generation, oxidative stress, and aging. *Free Radic Biol Med* *29*, 222-230.
- Cammack, R. (1995). Redox States and Potentials. In *Bioenergetics - A Practical Approach*, G.C.B.a.C.E. Cooper, ed. (Oxford: IRL Press), pp. 93-95.
- Carver, B.S. (2014). Strategies for targeting the androgen receptor axis in prostate cancer. *Drug Discov Today* *19*, 1493-1497.
- Chacinska, A., Pfannschmidt, S., Wiedemann, N., Kozjak, V., Sanjuan Szklarz, L.K., Schulze-Specking, A., Truscott, K.N., Guiard, B., Meisinger, C., and Pfanner, N. (2004). Essential role of Mia40 in import and assembly of mitochondrial intermembrane space proteins. *Embo J* *23*, 3735-3746.
- Chen, C.J., Fu, Y.C., Yu, W., and Wang, W. (2013). SIRT3 protects cardiomyocytes from oxidative stress-mediated cell death by activating NF-kappaB. *Biochem Biophys Res Commun* *430*, 798-803.
- Cheng, T.C., Hong, C., Akey, I.V., Yuan, S., and Akey, C.W. (2016). A near atomic structure of the active human apoptosome. *Elife* *5*.
- Cherney, M.M., Junior, C.C., and Bowler, B.E. (2013). Mutation of trimethyllysine 72 to alanine enhances His79-heme-mediated dynamics of iso-1-cytochrome c. *Biochemistry* *52*, 837-846.
- Choudhary, C., Kumar, C., Gnad, F., Nielsen, M.L., Rehman, M., Walther, T.C., Olsen, J.V., and Mann, M. (2009). Lysine acetylation targets protein complexes and co-regulates major cellular functions. *Science* *325*, 834-840.

Cohen, T.J., Guo, J.L., Hurtado, D.E., Kwong, L.K., Mills, I.P., Trojanowski, J.Q., and Lee, V.M. (2011). The acetylation of tau inhibits its function and promotes pathological tau aggregation. *Nat Commun* 2, 252.

Dabir, D.V., Leverich, E.P., Kim, S.K., Tsai, F.D., Hirasawa, M., Knaff, D.B., and Koehler, C.M. (2007). A role for cytochrome c and cytochrome c peroxidase in electron shuttling from Erv1. *EMBO J* 26, 4801-4811.

Dalmonte, M.E., Forte, E., Genova, M.L., Giuffre, A., Sarti, P., and Lenaz, G. (2009). Control of respiration by cytochrome c oxidase in intact cells: role of the membrane potential. *J Biol Chem* 284, 32331-32335.

Dickerson, R., and Timkovich, R. (1975). Cytochrome c. In *The Enzymes*, P. Boyer, ed. (New York: Academic Press), pp. 397-472.

Dumont, M.E., Cardillo, T.S., Hayes, M.K., and Sherman, F. (1991). Role of cytochrome c heme lyase in mitochondrial import and accumulation of cytochrome c in *Saccharomyces cerevisiae*. *Mol Cell Biol* 11, 5487-5496.

Fan, J., Shan, C., Kang, H.B., Elf, S., Xie, J., Tucker, M., Gu, T.L., Aguiar, M., Lonning, S., Chen, H., *et al.* (2014). Tyr phosphorylation of PDP1 toggles recruitment between ACAT1 and SIRT3 to regulate the pyruvate dehydrogenase complex. *Mol Cell* 53, 534-548.

Farooqui, J., DiMaria, P., Kim, S., and Paik, W.K. (1981). Effect of methylation on the stability of cytochrome c of *Saccharomyces cerevisiae* in vivo. *J Biol Chem* 256, 5041-5045.

Giorgio, M., Migliaccio, E., Orsini, F., Paolucci, D., Moroni, M., Contursi, C., Pelliccia, G., Luzi, L., Minucci, S., Marcaccio, M., *et al.* (2005). Electron transfer between cytochrome c and p66Shc generates reactive oxygen species that trigger mitochondrial apoptosis. *Cell* 122, 221-233.

Gorsky, M.K., Burnouf, S., Dols, J., Mandelkow, E., and Partridge, L. (2016). Acetylation mimic of lysine 280 exacerbates human Tau neurotoxicity in vivo. *Sci Rep* 6, 22685.

Green, D.R. (2000). Apoptotic pathways: paper wraps stone blunts scissors. *Cell* 102, 1-4.

Grillon, J.M., Johnson, K.R., Kotlo, K., and Danziger, R.S. (2012). Non-histone lysine acetylated proteins in heart failure. *Biochim Biophys Acta* 1822, 607-614.

Guan, K.L., and Xiong, Y. (2011). Regulation of intermediary metabolism by protein acetylation. *Trends Biochem Sci* 36, 108-116.

Han, D., Canali, R., Rettori, D., and Kaplowitz, N. (2003). Effect of glutathione depletion on sites and topology of superoxide and hydrogen peroxide production in mitochondria. *Mol Pharmacol* 64, 1136-1144.

Han, D., Williams, E., and Cadenas, E. (2001). Mitochondrial respiratory chain-dependent generation of superoxide anion and its release into the intermembrane space. *Biochem J* 353, 411-416.

Hao, Z., Duncan, G.S., Chang, C.C., Elia, A., Fang, M., Wakeham, A., Okada, H., Calzascia, T., Jang, Y., You-Ten, A., *et al.* (2005). Specific ablation of the apoptotic functions of cytochrome C reveals a differential requirement for cytochrome C and Apaf-1 in apoptosis. *Cell* 121, 579-591.

Harbitz, E., and Andersson, K.K. (2011). Cytochrome c-554 from *Methylosporium OB3b*; a protein that belongs to the cytochrome c2 family and exhibits a HALS-Type EPR signal. *PLoS One* 6, e22014.

Hebert, A.S., Dittenhafer-Reed, K.E., Yu, W., Bailey, D.J., Selen, E.S., Boersma, M.D., Carson, J.J., Tonelli, M., Balloon, A.J., Higbee, A.J., *et al.* (2013). Calorie restriction and SIRT3 trigger global reprogramming of the mitochondrial protein acetylome. *Mol Cell* 49, 186-199.

Hell, K. (2008). The Erv1-Mia40 disulfide relay system in the intermembrane space of mitochondria. *Biochim Biophys Acta* 1783, 601-609.

Herrmann, J.M., and Riemer, J. (2012). Mitochondrial disulfide relay: redox-regulated protein import into the intermembrane space. *J Biol Chem* 287, 4426-4433.

Hinkle, P.C., Kumar, M.A., Resetar, A., and Harris, D.L. (1991). Mechanistic stoichiometry of mitochondrial oxidative phosphorylation. *Biochemistry* 30, 3576-3582.

Holzschu, D., Principio, L., Conklin, K.T., Hickey, D.R., Short, J., Rao, R., McLendon, G., and Sherman, F. (1987). Replacement of the invariant lysine 77 by arginine in yeast iso-1-cytochrome c results in enhanced and normal activities in vitro and in vivo. *J Biol Chem* 262, 7125-7131.

Horton, J.L., Martin, O.J., Lai, L., Riley, N.M., Richards, A.L., Vega, R.B., Leone, T.C., Pagliarini, D.J., Muoio, D.M., Bedi, K.C., Jr., *et al.* (2016). Mitochondrial protein hyperacetylation in the failing heart. *JCI Insight* 2.

Hosp, F., Lassowskat, I., Santoro, V., De Vleeschauwer, D., Fliegner, D., Redestig, H., Mann, M., Christian, S., Hannah, M.A., and Finkemeier, I. (2017). Lysine acetylation in mitochondria: From inventory to function. *Mitochondrion* 33, 58-71.

Hüttemann, M., Doan, J.W., Goustin, A.S., Sinkler, C., Mahapatra, G., Shay, J., Liu, J., Elbaz, H.A., Aras, S., Grossman, L.I., *et al.* (2014). Regulation of cytochrome c in respiration, apoptosis, neurodegeneration and cancer: The good, the bad and the ugly. In *Cytochromes b and c*, R. Thom, ed. (Hauppauge NY: Nova Science Publishers, Inc.), pp. 1-38.

Hüttemann, M., Jaradat, S., and Grossman, L.I. (2003). Cytochrome c oxidase of mammals contains a testes-specific isoform of subunit VIIb – the counterpart to testes-specific cytochrome c? *Mol Reprod Dev* 66, 8-16.

Hüttemann, M., Pecina, P., Rainbolt, M., Sanderson, T.H., Kagan, V.E., Samavati, L., Doan, J.W., and Lee, I. (2011). The multiple functions of cytochrome c and their regulation in life and death decisions of the mammalian cell: From respiration to apoptosis. *Mitochondrion* 11, 369-381.

Iverson, S.L., and Orrenius, S. (2004). The cardiolipin-cytochrome c interaction and the mitochondrial regulation of apoptosis. *Arch Biochem Biophys* 423, 37-46.

Jastroch, M., Divakaruni, A.S., Mookerjee, S., Treberg, J.R., and Brand, M.D. (2010). Mitochondrial proton and electron leaks. *Essays Biochem* 47, 53-67.

Jeong, H., Then, F., Melia, T.J., Jr., Mazzulli, J.R., Cui, L., Savas, J.N., Voisine, C., Paganetti, P., Tanese, N., Hart, A.C., *et al.* (2009). Acetylation targets mutant huntingtin to autophagosomes for degradation. *Cell* 137, 60-72.

Kabsch, W. (2010). Xds. *Acta Crystallogr D Biol Crystallogr* 66, 125-132.

Kadenbach, B., Arnold, S., Lee, I., and Hüttemann, M. (2004). The possible role of cytochrome c oxidase in stress-induced apoptosis and degenerative diseases. *Biochim Biophys Acta* 1655, 400-408.

Kagan, V.E., Borisenko, G.G., Tyurina, Y.Y., Tyurin, V.A., Jiang, J., Potapovich, A.I., Kini, V., Amoscato, A.A., and Fujii, Y. (2004). Oxidative lipidomics of apoptosis: redox catalytic interactions of cytochrome c with cardiolipin and phosphatidylserine. *Free Radic Biol Med* 37, 1963-1985.

Kagan, V.E., Tyurin, V.A., Jiang, J., Tyurina, Y.Y., Ritow, V.B., Amoscato, A.A., Osipov, A.N., Belikova, N.A., Kapralov, A.A., Kini, V., *et al.* (2005). Cytochrome c acts as a cardiolipin oxygenase required for release of proapoptotic factors. *Nature Chem Biol* 1, 223-232.

Kaim, G., and Dimroth, P. (1999). ATP synthesis by F-type ATP synthase is obligatorily dependent on the transmembrane voltage. *Embo J* 18, 4118-4127.

Kim, C.S., Kueppers, F., Dimaria, P., Farooqui, J., Kim, S., and Paik, W.K. (1980). Enzymatic trimethylation of residue-72 lysine in cytochrome c. Effect on the total structure. *Biochim Biophys Acta* 622, 144-150.

Kim, S.C., Sprung, R., Chen, Y., Xu, Y., Ball, H., Pei, J., Cheng, T., Kho, Y., Xiao, H., Xiao, L., *et al.* (2006). Substrate and functional diversity of lysine acetylation revealed by a proteomics survey. *Mol Cell* 23, 607-618.

Kluck, R.M., Ellerby, L.M., Ellerby, H.M., Naiem, S., Yaffe, M.P., Margoliash, E., Bredesen, D., Mauk, A.G., Sherman, F., and Newmeyer, D.D. (2000). Determinants of cytochrome c pro-apoptotic activity. The role of lysine 72 trimethylation. *J Biol Chem* 275, 16127-16133.

Konig, A.C., Hartl, M., Boersema, P.J., Mann, M., and Finkemeier, I. (2014). The mitochondrial lysine acetylome of Arabidopsis. *Mitochondrion* 19 Pt B, 252-260.

Korshunov, S.S., Krasnikov, B.F., Pereverzev, M.O., and Skulachev, V.P. (1999). The antioxidant functions of cytochrome c. *FEBS Lett* 462, 192-198.

Krippner, A., Matsuno-Yagi, A., Gottlieb, R.A., and Babior, B.M. (1996). Loss of function of cytochrome c in Jurkat cells undergoing fas-mediated apoptosis. *J Biol Chem* 271, 21629-21636.

Kwon, M., Chong, S., Han, S., and Kim, K. (2003). Oxidative stresses elevate the expression of cytochrome c peroxidase in *Saccharomyces cerevisiae*. *Biochim Biophys Acta* 1623, 1-5.

Lee, C.F., and Tian, R. (2015). Mitochondrion as a Target for Heart Failure Therapy- Role of Protein Lysine Acetylation. *Circ J* 79, 1863-1870.

Lee, I., Salomon, A.R., Yu, K., Doan, J.W., Grossman, L.I., and Hüttemann, M. (2006). New prospects for an old enzyme: mammalian cytochrome c is tyrosine-phosphorylated in vivo. *Biochemistry* 45, 9121-9128.

Lee, I., Salomon, A.R., Yu, K., Samavati, L., Pecina, P., Pecinova, A., and Hüttemann, M. (2009). Isolation of regulatory-competent, phosphorylated cytochrome c oxidase. *Methods Enzymol* 457, 193-210.

Li, H., Kolluri, S.K., Gu, J., Dawson, M.I., Cao, X., Hobbs, P.D., Lin, B., Chen, G., Lu, J., Lin, F., *et al.* (2000a). Cytochrome c release and apoptosis induced by mitochondrial targeting of nuclear orphan receptor TR3. *Science* 289, 1159-1164.

Li, K., Li, Y., Shelton, J.M., Richardson, J.A., Spencer, E., Chen, Z.J., Wang, X., and Williams, R.S. (2000b). Cytochrome c deficiency causes embryonic lethality and attenuates stress-induced apoptosis. *Cell* 101, 389-399.

Lin, R., Tao, R., Gao, X., Li, T., Zhou, X., Guan, K.L., Xiong, Y., and Lei, Q.Y. (2013). Acetylation stabilizes ATP-citrate lyase to promote lipid biosynthesis and tumor growth. *Mol Cell* 51, 506-518.

Lin, R., Zhou, X., Huang, W., Zhao, D., Lv, L., Xiong, Y., Guan, K.L., and Lei, Q.Y. (2014). Acetylation control of cancer cell metabolism. *Curr Pharm Des* 20, 2627-2633.

Liu, S.S. (1999). Cooperation of a "reactive oxygen cycle" with the Q cycle and the proton cycle in the respiratory chain--superoxide generating and cycling mechanisms in mitochondria. *J Bioenerg Biomembr* 31, 367-376.

Liu, X., Kim, C.N., Yang, J., Jemmerson, R., and Wang, X. (1996). Induction of apoptotic program in cell-free extracts: requirement for dATP and cytochrome c. *Cell* 86, 147-157.

Liu, Z., Lin, H., Ye, S., Liu, Q.Y., Meng, Z., Zhang, C.M., Xia, Y., Margoliash, E., Rao, Z., and Liu, X.J. (2006). Remarkably high activities of testicular cytochrome c in destroying reactive oxygen species and in triggering apoptosis. *Proc Natl Acad Sci USA* *103*, 8965-8970.

Lundby, A., Lage, K., Weinert, B.T., Bekker-Jensen, D.B., Secher, A., Skovgaard, T., Kelstrup, C.D., Dmytriiev, A., Choudhary, C., Lundby, C., *et al.* (2012). Proteomic analysis of lysine acetylation sites in rat tissues reveals organ specificity and subcellular patterns. *Cell Rep* *2*, 419-431.

Lv, L., Li, D., Zhao, D., Lin, R., Chu, Y., Zhang, H., Zha, Z., Liu, Y., Li, Z., Xu, Y., *et al.* (2011). Acetylation targets the M2 isoform of pyruvate kinase for degradation through chaperone-mediated autophagy and promotes tumor growth. *Mol Cell* *42*, 719-730.

Mahapatra, G., Varughese, A., Ji, Q., Lee, I., Liu, J., Vaishnav, A., Sinkler, C., Kapralov, A.A., Moraes, C.T., Sanderson, T.H., *et al.* (2017). Phosphorylation of Cytochrome c Threonine 28 Regulates Electron Transport Chain Activity in Kidney: IMPLICATIONS FOR AMP KINASE. *J Biol Chem* *292*, 64-79.

Michan, S. (2013). Acetylome regulation by sirtuins in the brain: from normal physiology to aging and pathology. *Curr Pharm Des* *19*, 6823-6838.

Nemoto, S., Combs, C.A., French, S., Ahn, B.H., Fergusson, M.M., Balaban, R.S., and Finkel, T. (2006). The mammalian longevity-associated gene product p66shc regulates mitochondrial metabolism. *J Biol Chem* *281*, 10555-10560.

Nicholls, D.G., and Ferguson, S.J. (1992). *Bioenergetics 2* (London, San Diego: Academic Press Limited).

Pahllich, S., Zakaryan, R.P., and Gehring, H. (2006). Protein arginine methylation: Cellular functions and methods of analysis. *Biochim Biophys Acta* *1764*, 1890-1903.

Paik, W.K., Cho, Y.B., Frost, B., and Kim, S. (1989). Cytochrome c methylation. *Biochem Cell Biol* *67*, 602-611.

Paik, W.K., Paik, D.C., and Kim, S. (2007). Historical review: the field of protein methylation. *Trends Biochem Sci* *32*, 146-152.

Park, K.S., Frost, B., Tuck, M., Ho, L.L., Kim, S., and Paik, W.K. (1987). Enzymatic methylation of in vitro synthesized apocytochrome c enhances its transport into mitochondria. *J Biol Chem* *262*, 14702-14708.

Patel, C.N., Lind, M.C., and Pielak, G.J. (2001). Characterization of horse cytochrome c expressed in *Escherichia coli*. *Protein Expr Purif* *22*, 220-224.

Pecina, P., Borisenko, G.G., Belikova, N.A., Tyurina, Y.Y., Pecinova, A., Lee, I., Samhan-Arias, A.K., Przyklenk, K., Kagan, V.E., and Hüttemann, M. (2010). Phosphomimetic substitution of cytochrome c tyrosine 48 decreases respiration and binding to cardiolipin and abolishes ability to trigger downstream caspase activation. *Biochemistry* *49*, 6705-6714.

Pereverzev, M.O., Vygodina, T.V., Konstantinov, A.A., and Skulachev, V.P. (2003). Cytochrome c, an ideal antioxidant. *Biochem Soc Trans* *31*, 1312-1315.

Pinton, P., Rimessi, A., Marchi, S., Orsini, F., Migliaccio, E., Giorgio, M., Contursi, C., Minucci, S., Mantovani, F., Wieckowski, M.R., *et al.* (2007). Protein kinase C beta and prolyl isomerase 1 regulate mitochondrial effects of the life-span determinant p66Shc. *Science* *315*, 659-663.

Polastro, E., Schneck, A.G., Leonis, J., Kim, S., and Paik, W.K. (1978). Cytochrome c methylation. *Int J Biochem* *9*, 795-801.

Pollock, W.B., Rosell, F.I., Twitchett, M.B., Dumont, M.E., and Mauk, A.G. (1998). Bacterial expression of a mitochondrial cytochrome c. Trimethylation of lys72 in yeast iso-1-cytochrome c and the alkaline conformational transition. *Biochemistry* 37, 6124-6131.

Rehling, P., Wiedemann, N., Pfanner, N., and Truscott, K.N. (2001). The mitochondrial import machinery for preproteins. *Crit Rev Biochem Mol Biol* 36, 291-336.

Schlame, M., Rua, D., and Greenberg, M.L. (2000). The biosynthesis and functional role of cardiolipin. *Prog Lipid Res* 39, 257-288.

Slee, E.A., Harte, M.T., Kluck, R.M., Wolf, B.B., Casiano, C.A., Newmeyer, D.D., Wang, H.G., Reed, J.C., Nicholson, D.W., Alnemri, E.S., *et al.* (1999). Ordering the cytochrome c-initiated caspase cascade: hierarchical activation of caspases-2, -3, -6, -7, -8, and -10 in a caspase-9-dependent manner. *J Cell Biol* 144, 281-292.

Smith-Hammond, C.L., Hoyos, E., and Miernyk, J.A. (2014). The pea seedling mitochondrial Nepsilon-lysine acetylome. *Mitochondrion* 19 Pt B, 154-165.

Stock, D., Leslie, A.G., and Walker, J.E. (1999). Molecular architecture of the rotary motor in ATP synthase. *Science* 286, 1700-1705.

Sun, L., Xiao, L., Nie, J., Liu, F.Y., Ling, G.H., Zhu, X.J., Tang, W.B., Chen, W.C., Xia, Y.C., Zhan, M., *et al.* (2010). p66Shc mediates high glucose and angiotensin II induced oxidative stress renal tubular injury via mitochondrial dependent apoptotic pathway. *Am J Physiol Renal Physiol* 299, F1014-1012.

Turrens, J.F., Alexandre, A., and Lehninger, A.L. (1985). Ubisemiquinone is the electron donor for superoxide formation by complex III of heart mitochondria. *Arch Biochem Biophys* 237, 408-414.

Vadvalkar, S.S., Baily, C.N., Matsuzaki, S., West, M., Tesiram, Y.A., and Humphries, K.M. (2013). Metabolic inflexibility and protein lysine acetylation in heart mitochondria of a chronic model of type 1 diabetes. *Biochem J* 449, 253-261.

Vander Heiden, M.G., Cantley, L.C., and Thompson, C.B. (2009). Understanding the Warburg effect: the metabolic requirements of cell proliferation. *Science* 324, 1029-1033.

Vempati, U.D., Diaz, F., Barrientos, A., Narisawa, S., Mian, A.M., Millan, J.L., Boise, L.H., and Moraes, C.T. (2007). Role of cytochrome C in apoptosis: increased sensitivity to tumor necrosis factor alpha is associated with respiratory defects but not with lack of cytochrome C release. *Mol Cell Biol* 27, 1771-1783.

Villani, G., and Attardi, G. (1997). In vivo control of respiration by cytochrome c oxidase in wild-type and mitochondrial DNA mutation-carrying human cells. *Proc Natl Acad Sci U S A* 94, 1166-1171.

Villani, G., Greco, M., Papa, S., and Attardi, G. (1998). Low reserve of cytochrome c oxidase capacity in vivo in the respiratory chain of a variety of human cell types. *J Biol Chem* 273, 31829-31836.

Volkov, A.N., Nicholls, P., and Worrall, J.A. (2011). The complex of cytochrome c and cytochrome c peroxidase: the end of the road? *Biochim Biophys Acta* 1807, 1482-1503.

Vonrhein, C., Flensburg, C., Keller, P., Sharff, A., Smart, O., Paciorek, W., Womack, T., and Bricogne, G. (2011). Data processing and analysis with the autoPROC toolbox. *Acta Crystallogr D Biol Crystallogr* 67, 293-302.

Wagner, G. (2005). Ending the prolonged life of cancer cells. *Nat Chem Biol* 1, 8-9.

Wang, X. (2001). The expanding role of mitochondria in apoptosis. *Genes Dev* 15, 2922-2933.

Wang, Z.B., Li, M., Zhao, Y., and Xu, J.X. (2003). Cytochrome c is a hydrogen peroxide scavenger in mitochondria. *Protein Pept Lett* *10*, 247-253.

Warburg, O. (1956). On the origin of cancer cells. *Science* *123*, 309-314.

Warburg, O., Posener, K., and Negelein, E. (1924). Über den Stoffwechsel der Carcinomzelle. *Biochem Z* *152*, 309-344.

Ward, P.S., and Thompson, C.B. (2012). Metabolic reprogramming: a cancer hallmark even warburg did not anticipate. *Cancer Cell* *21*, 297-308.

Weinberg, S.E., and Chandel, N.S. (2015). Targeting mitochondria metabolism for cancer therapy. *Nat Chem Biol* *11*, 9-15.

Winter, D.L., Abeygunawardena, D., Hart-Smith, G., Erce, M.A., and Wilkins, M.R. (2015). Lysine methylation modulates the protein-protein interactions of yeast cytochrome C Cyc1p. *Proteomics* *15*, 2166-2176.

Yang, H., Zhou, L., Shi, Q., Zhao, Y., Lin, H., Zhang, M., Zhao, S., Yang, Y., Ling, Z.Q., Guan, K.L., *et al.* (2015). SIRT3-dependent GOT2 acetylation status affects the malate-aspartate NADH shuttle activity and pancreatic tumor growth. *EMBO J* *34*, 1110-1125.

Yu, H., Lee, I., Salomon, A.R., Yu, K., and Hüttemann, M. (2008). Mammalian liver cytochrome c is tyrosine-48 phosphorylated in vivo, inhibiting mitochondrial respiration. *Biochim Biophys Acta* *1777*, 1066-1071.

Zaidi, S., Hassan, M.I., Islam, A., and Ahmad, F. (2014). The role of key residues in structure, function, and stability of cytochrome-c. *Cell Mol Life Sci* *71*, 229-255.

Zhao, D., Zou, S.W., Liu, Y., Zhou, X., Mo, Y., Wang, P., Xu, Y.H., Dong, B., Xiong, Y., Lei, Q.Y., *et al.* (2013). Lysine-5 acetylation negatively regulates lactate dehydrogenase A and is decreased in pancreatic cancer. *Cancer Cell* *23*, 464-476.

Zhao, X., Leon, I.R., Bak, S., Mogensen, M., Wrzesinski, K., Hojlund, K., and Jensen, O.N. (2011). Phosphoproteome analysis of functional mitochondria isolated from resting human muscle reveals extensive phosphorylation of inner membrane protein complexes and enzymes. *Mol Cell Proteomics* *10*, M110 000299.

Zhou, M., Li, Y., Hu, Q., Bai, X.C., Huang, W., Yan, C., Scheres, S.H., and Shi, Y. (2015). Atomic structure of the apoptosome: mechanism of cytochrome c- and dATP-mediated activation of Apaf-1. *Genes Dev* *29*, 2349-2361.

ABSTRACT**THE EFFECT OF ACETYLATION OF CYTOCHROME *C* ON ITS FUNCTIONS IN
CANCER**

by

VIKTORIIA BAZYLIANSKA**May 2017****Advisor:** Dr. Maik Hüttemann**Major:** Biochemistry and Molecular Biology**Degree:** Master of Science

Prostate cancer is the second leading cause of cancer death among men in America. The progression of cancer goes along with the Warburg effect, a metabolic switch from depending primarily on mitochondrial respiration to glycolysis. In addition, cancer cells manage to evade apoptosis. Cell signaling, via posttranslational modifications (PTMs), is one of the most important means of regulation, and most commonly dysregulated in cancer. In prostate cancer, androgen signaling plays a crucial role in driving cell proliferation.

Mammalian Cytochrome *c* (Cyt c) is a multifunctional protein involved in cellular life and death decision. It is an essential component of the electron transport chain (ETC), where it shuttles electrons to cytochrome *c* oxidase (COX) to eventually generate ATP. Cyt c also functions as a trigger of apoptosis when released into the cytosol. However, its regulation is not well understood. Previously, it was shown that Cyt c can be posttranslationally modified and regulated by phosphorylation through cell signaling pathways, controlling the protein functions.

In this study, we demonstrated that development of prostate cancer causes changes in *Cytc* posttranslational modifications which in turn, alter the main protein functions, including respiration and apoptosis. The preliminary data demonstrated that human *Cytc* is acetylated on lysine 53 in eight independent castrate-resistant and -sensitive human tumor xenografts, suggesting that this is a cancer-specific modification. To characterize the functional effects, Lys-53 was mutated to the acetylmimetic glutamine, a non-acetylated arginine that carries a positive charge, and to the nonpolar isoleucine as an additional control. *Cytc* variants were overexpressed in bacteria and purified to homogeneity. COX activity, analyzed with purified *Cytc* variants, demonstrated that the acetylmimetic Lys53Gln *Cytc* showed reduced respiration compared to the nonacetylated WT. Remarkably, compared to WT, acetylmimetic Lys53Gln mutant was unable to trigger caspase-3 activity and hence, to induce apoptosis. This data suggests that the Lys-53 epitope is directly involved in the interaction between *Cytc* and Apaf-1. Our study shows that acetylmimetic Lys53Gln causes a reduction of peroxidase activity of *Cytc* compared to WT control, proving the results that Lys53Gln is incapable of triggering apoptosis. We observed that the redox potentials of the *Cytc* variants were in a range between the redox potential of complex III and IV, suggesting the ability of proteins to function properly, which was also confirmed by spectrophotometric analysis. We also showed that Lys53Gln *Cytc* mutant has a higher ability to degrade H₂O₂ and act as a stronger ROS scavenger compared to WT. Additionally, Lys53Gln *Cytc* mutant demonstrated a better capacity to accept electrons further supporting its role as ROS scavenger. In summary, our data suggest that cell signaling regulates cellular respiration and apoptosis via PTMs of *Cytc*, and suggest distinct regulation of *Cytc* in cancer.

AUTOBIOGRAPHICAL STATEMENT**EDUCATION:**

Master of Science - Biochemistry and Molecular Biology **May 2017**

Wayne State University, Detroit, MI,

Master of Science - Biotechnology with Honors **June 2015**

Taras Shevchenko National University of Kyiv, Kyiv, Ukraine

Bachelor of Science - Biology with Honors **June 2013**

Taras Shevchenko National University of Kyiv, Kyiv, Ukraine

HONORS AND AWARDS:

J. William Fulbright Foreign Scholarship Board (FFSB), *USA*

German Academic Exchange Service Scholarship (DAAD), *Germany*

Rector's Award, Taras Shevchenko National University of Kyiv, *Ukraine*

Scholarship and Award from the President of Ukraine, *Ukraine*

Ministry of Education Scholarship, *Ukraine*